

Experimental Results from the STAR Experiment at Relativistic Heavy Ion Collider



Lokesh Kumar
Panjab University Chandigarh

lokesh@pu.ac.in

Joint Institute for Nuclear Research (JINR),
Russia

1 December 2022



Outline

- Introduction
- Experimental Detail
- Results (from Beam Energy Scan)
- Summary



Outline

- Introduction
- Experimental Detail
- Results (from Beam Energy Scan)
- Summary



Goals of Relativistic Nuclear Collisions

- Search for Quark-Gluon Plasma (QGP) or partonic matter & study its properties
- Understand particle production mechanism
- Explore Quantum Chromodynamics (QCD) phase diagram: QCD phase boundary, first-order phase transition, QCD critical point

RHIC Beam Energy Scan Program (BES)

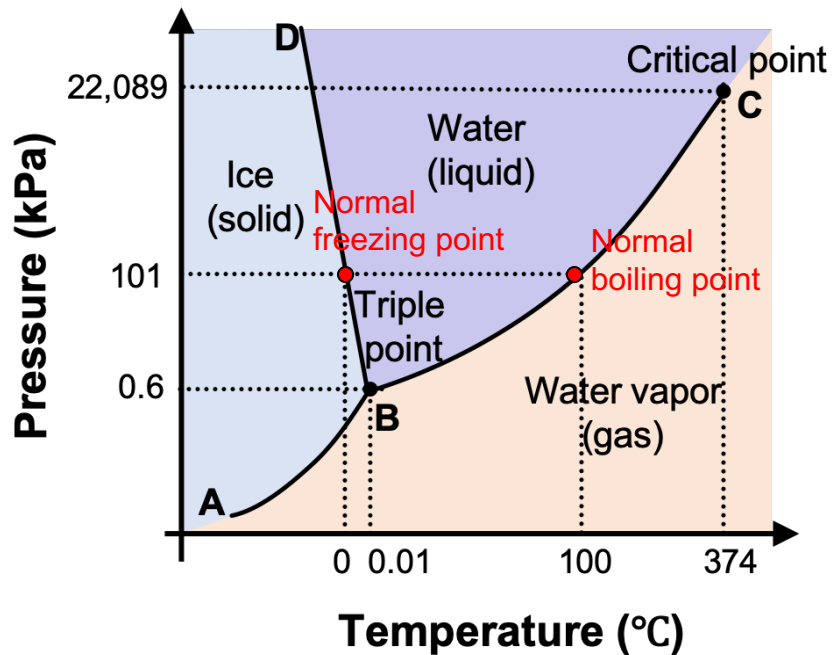
Year	Important Steps
2008	Proposal of RHIC Beam Energy Scan Program <i>Feasibility:</i> Au+Au 9.2 GeV test run [STAR: PRC 81, 024911 (2010)]
2010-14	First phase of BES (BES-I) [Many interesting results]
2018-21	Second phase (BES-II) [Data analysis ongoing]



Phase Structure of Matter

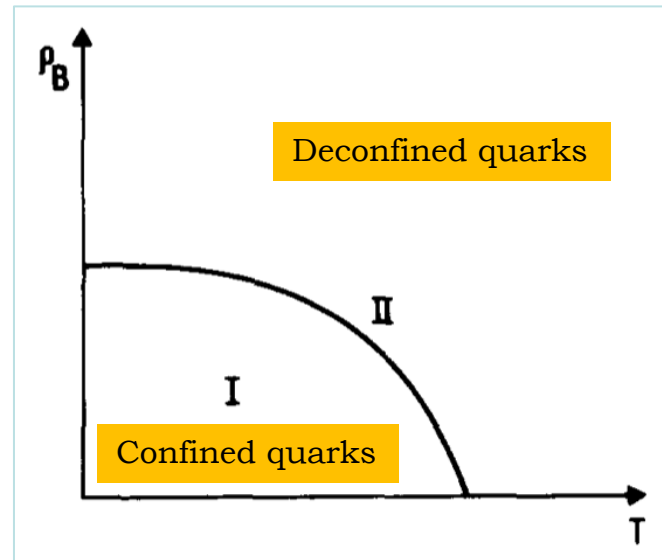
Phase Diagram: How the matter (re)organizes itself under given degrees of freedom

Phase Diagram of Water (QED):



Well established!

Phase Diagram of Strong interactions (QCD):



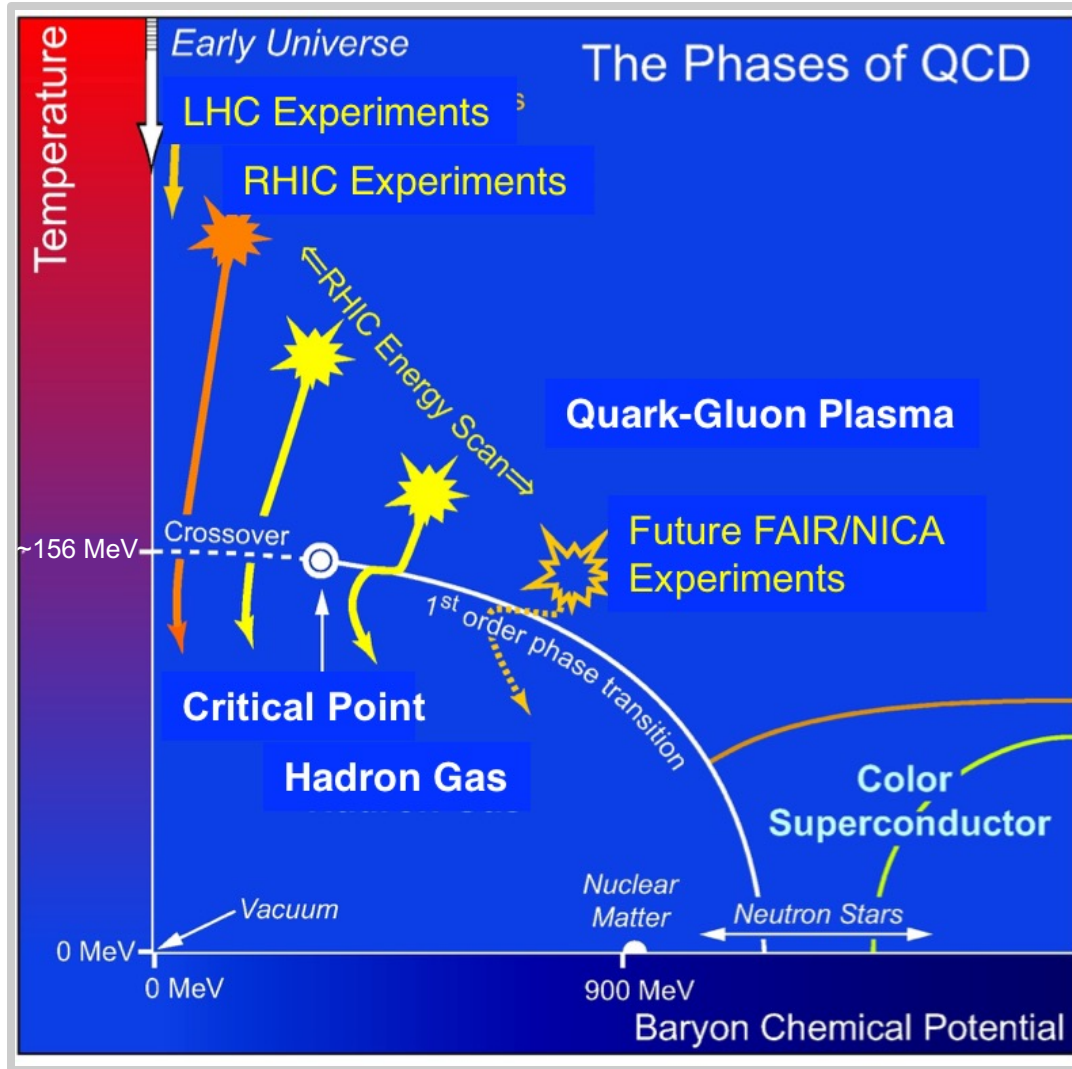
N. Cabbibo and G. Parisi, Phys. Lett. 59B, 1 (1975).

One of the initial conjectured QCD phase diagrams

Partially established!



QCD Phase Diagram



- Phase diagram of strongly interacting matter
- Plotted between temperature (T) and baryon chemical potential (μ_B)

Rich phase structure:

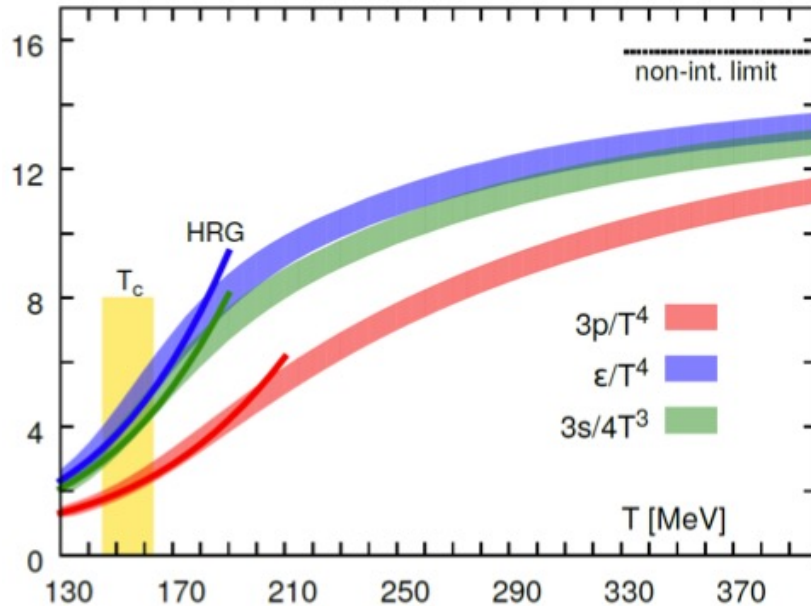
- Phase boundary
- Critical point
- Hadron gas
- Quark Gluon Plasma
- ...

$$(T, \mu_B) = F(\sqrt{s_{NN}})$$



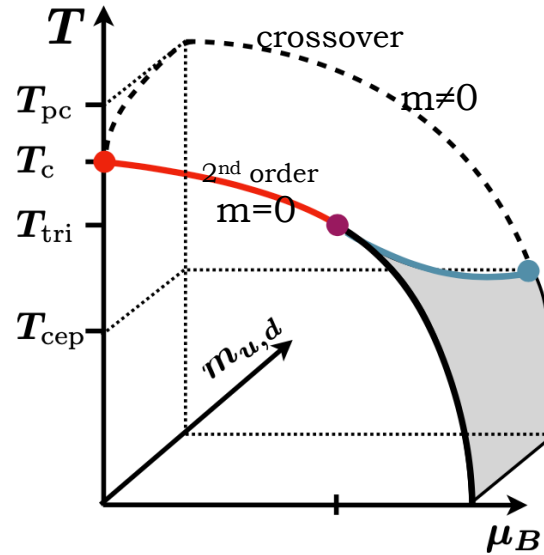
Lattice QCD Theory

Theory predicts a phase transition from Hadron gas to QGP at high temperature



HotQCD: A. Bazavov et al., PRD90, 094503 (2014)

Continuous crossover ($T \sim 150$ MeV) from HRG at low temperatures to QGP at high temperatures



F. Karsch, PoS CORFU2018 (2019)

Hot QCD :
PLB 795, 15 (2019);
PRL 123, 062002 (2019)

QCD transition temperature ($m \neq 0$):
 $T_{PC} = 156.5 \pm 1.5$ MeV

Chiral transition temperature ($m = 0$):
 $T_C = 132^{+3}_{-6}$ MeV

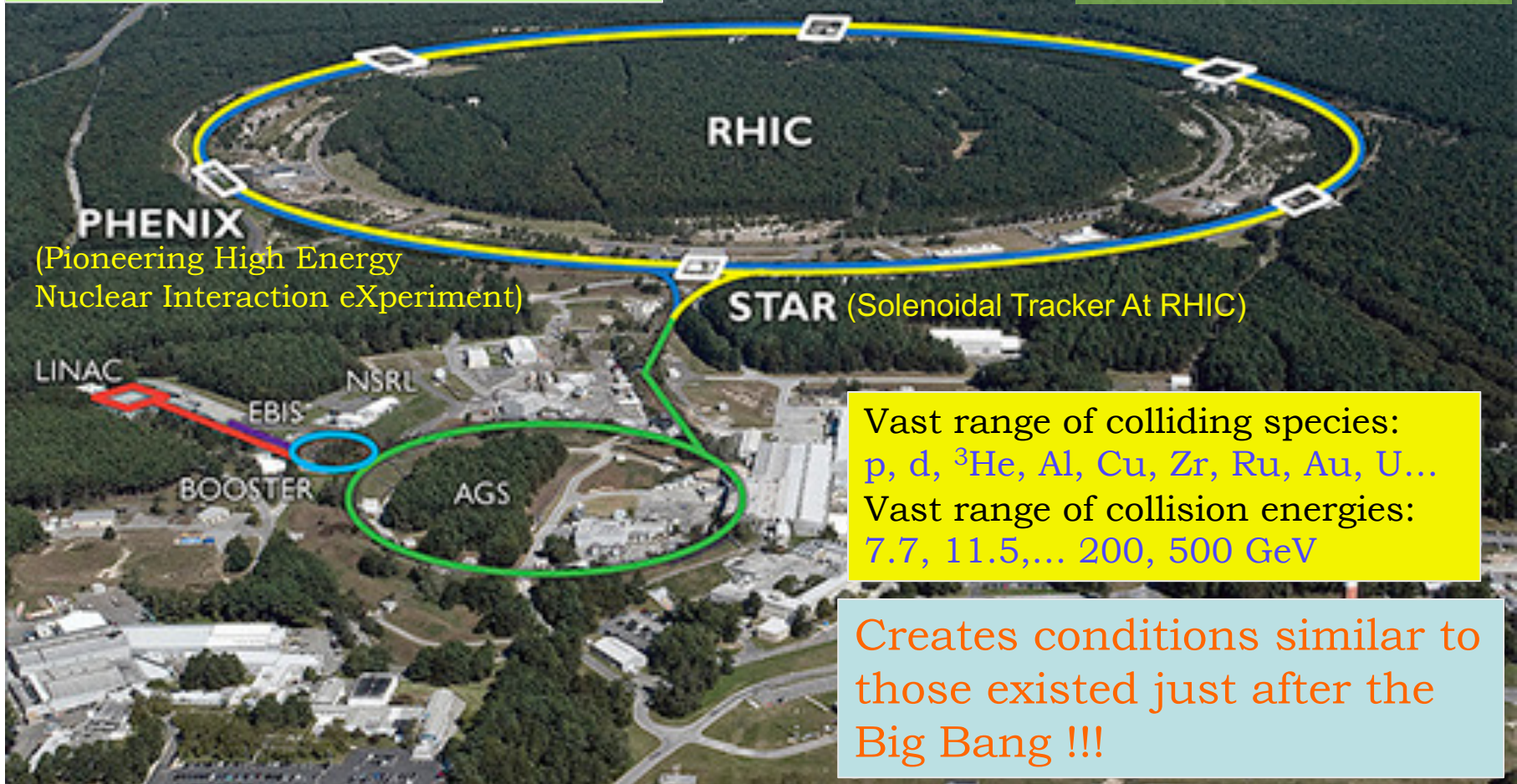
QCD critical end point ($m \neq 0, \mu_B \neq 0$):
 $T_{CEP} < T_C$ and $\mu_B^{CEP} \gtrsim 3T_C$



Relativistic Heavy-Ion Collider

(BNL, Upton, Long Island, USA)

Circumference: 3.8 km



Vast range of colliding species:
p, d, ^3He , Al, Cu, Zr, Ru, Au, U...
Vast range of collision energies:
7.7, 11.5,... 200, 500 GeV

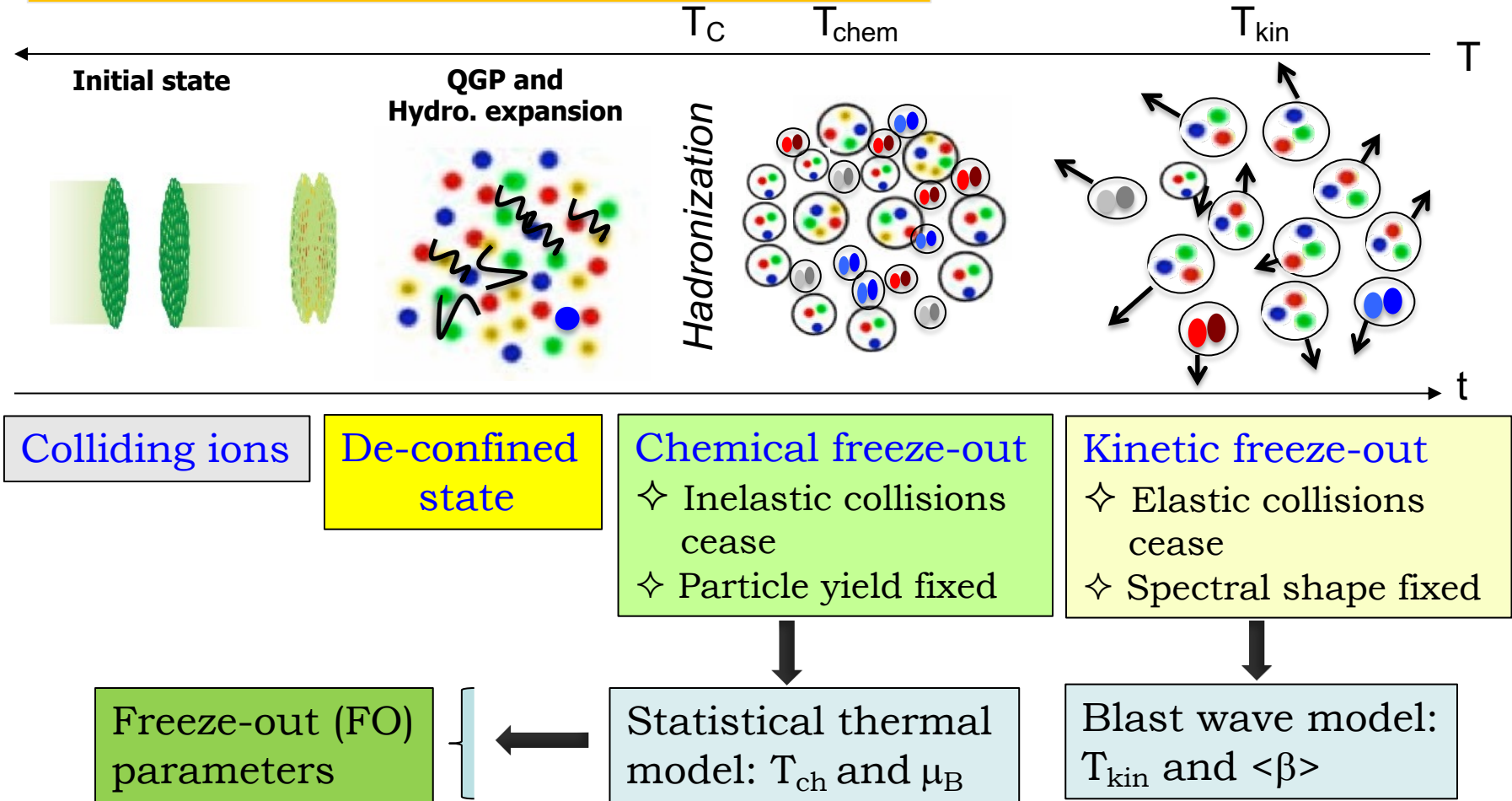
Creates conditions similar to
those existed just after the
Big Bang !!!

World's most versatile Collider Machine!



Evolution of Heavy-Ion Collisions

Time Evolution of Heavy-ion Collisions:



Parameters give information of QCD phase diagram and particle production

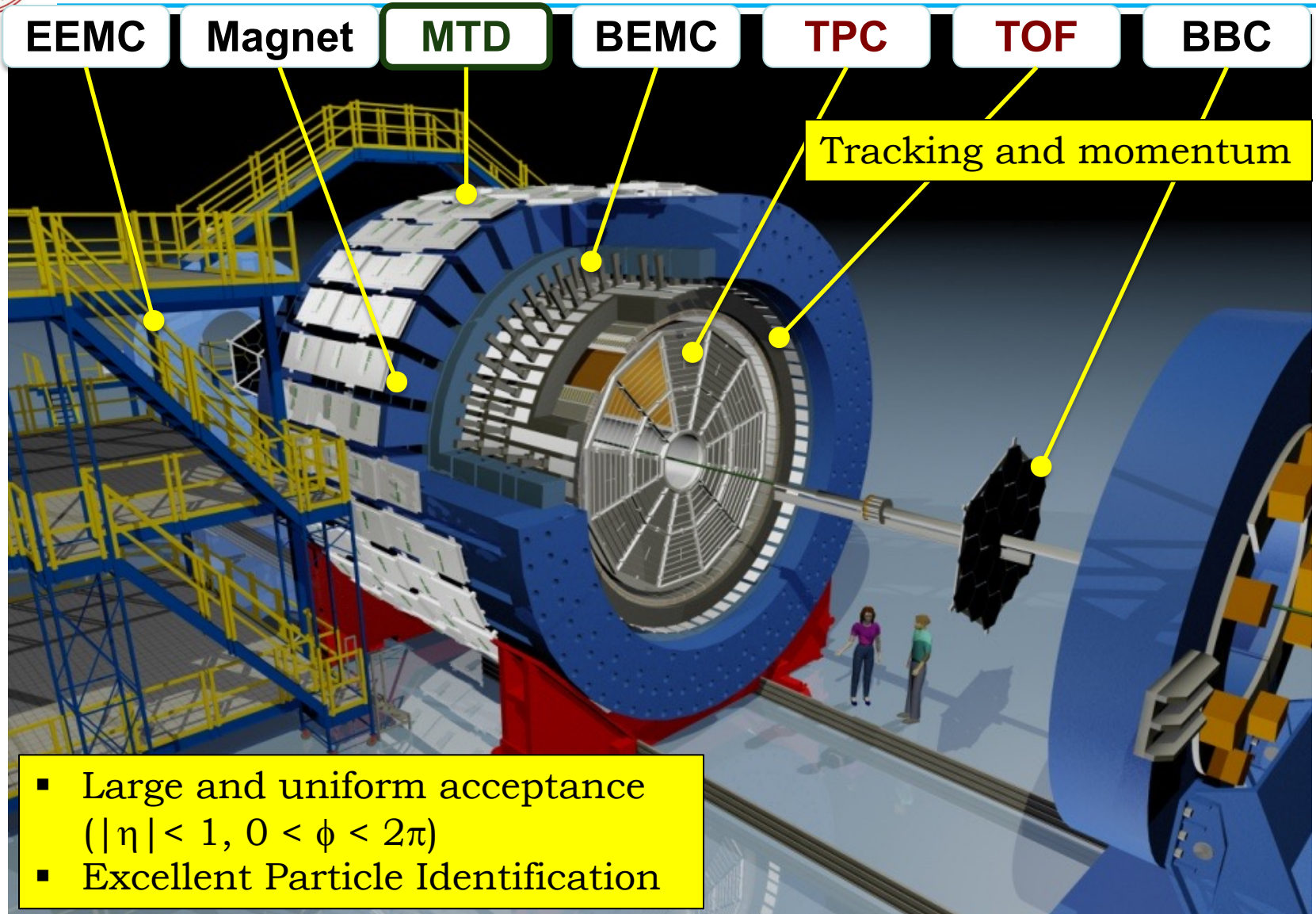


Outline

- Introduction
- Experimental Detail
- Results (from Beam Energy Scan)
- Summary



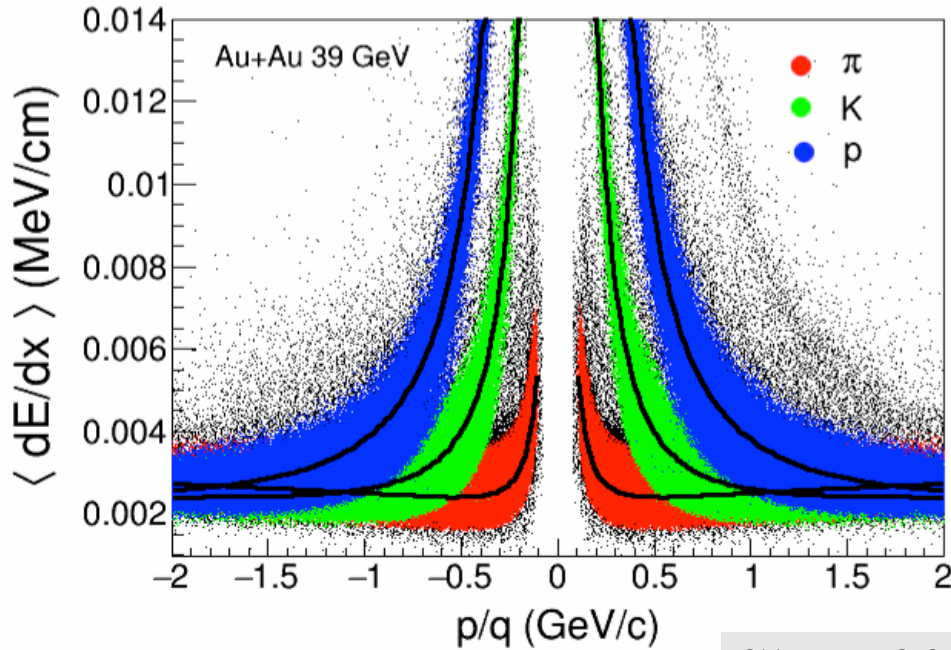
The STAR Experiment





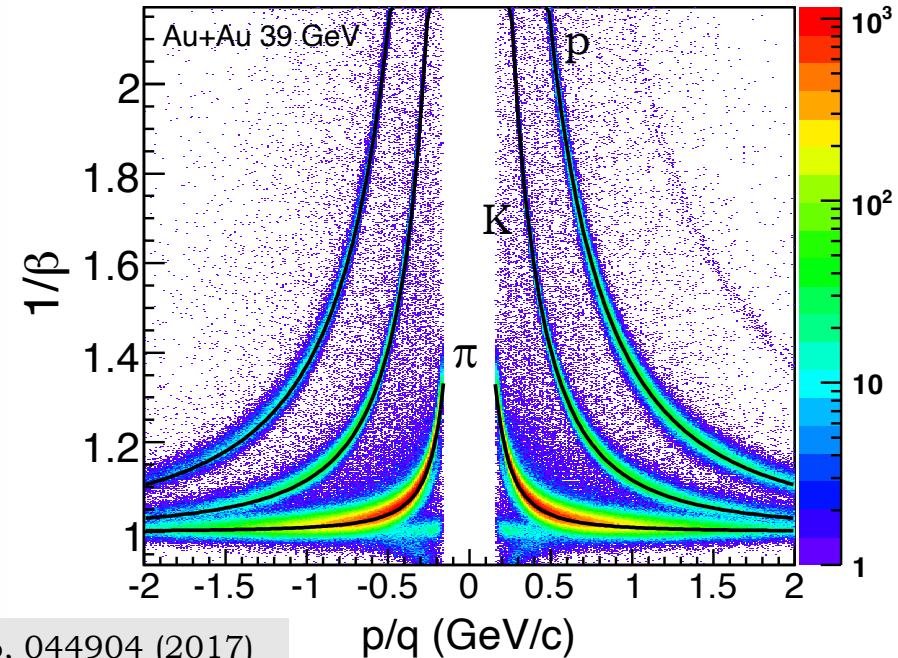
Particle Identification

TPC



π, K, p

TPC+TOF



STAR: PRC 96, 044904 (2017)

Ionization energy loss:

$$\begin{aligned}
 - \langle dE/dx \rangle &\sim A / \beta^2 \\
 &= A (1 + \mathbf{m}^2 / p^2)
 \end{aligned}$$

Time of flight:

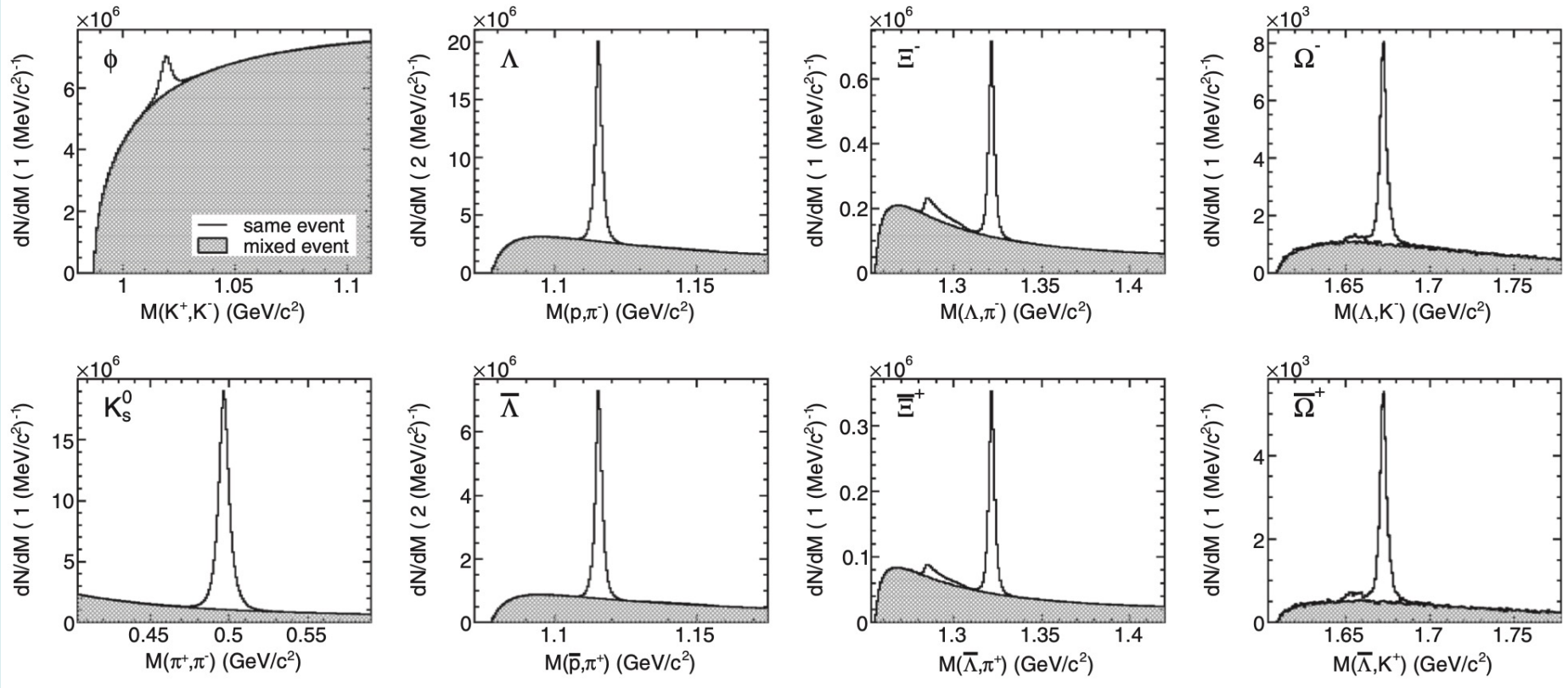
$$\begin{aligned}
 \langle \tau \rangle &= L / \beta \\
 &= L (1 + \mathbf{m}^2 / p^2)^{1/2}
 \end{aligned}$$



Particle Identification

Strange Hadrons and Resonance

Decay topology and invariant mass technique

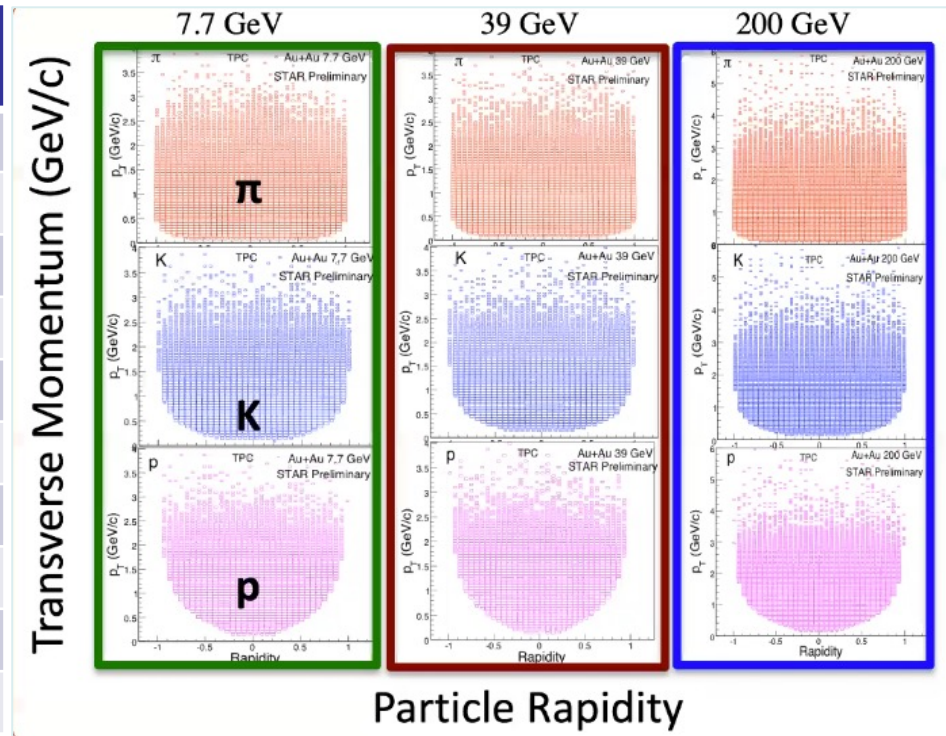


STAR: Phys. Rev. C 88, 014902 (2013)



Data Set BES-I (2010-2017)

$\sqrt{s_{NN}}$ (GeV)	Events (10^6)	Year	μ_B (MeV)	T_{ch} (MeV)
200	238	2010	25	166
62.4	46	2010	73	165
54.4	1200	2017	83	165
39	86	2010	112	164
27	30	2011	156	162
19.6	15	2011	206	160
14.5	13	2011	264	156
11.5	7	2010	316	152
7.7	4	2010	420	140
3.0	250	2018	~720	~80



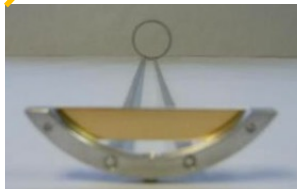
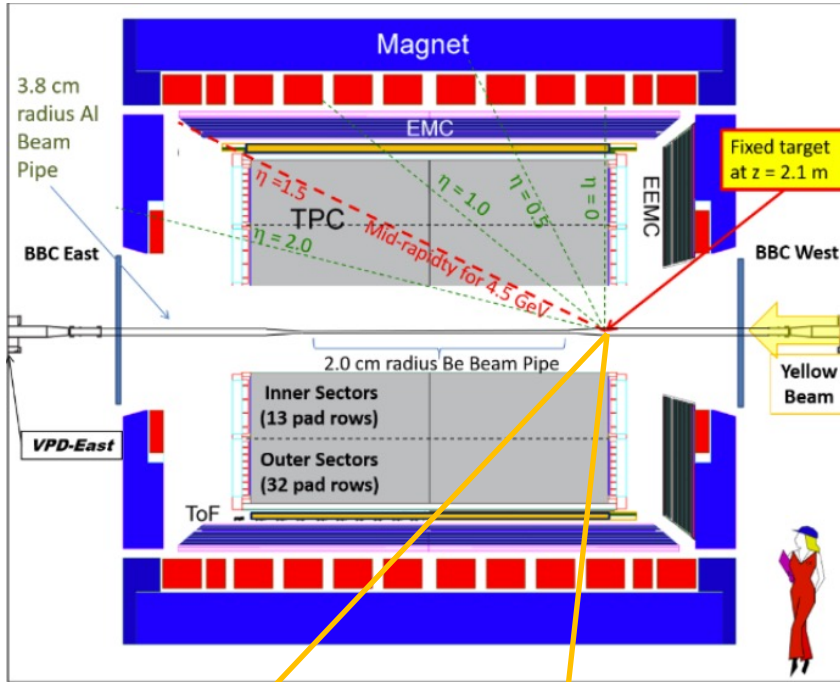
(μ_B, T_{ch}) : J. Cleymans et al. PRC 73, 034905 (2006)

- Covers big region of the QCD phase diagram ($\mu_B = 25 - 720$ MeV)
- Large and uniform acceptance across energies (important for fluctuation analyses) – advantage in collider experiments!

Fixed Target: Advantage of higher rates and higher statistics



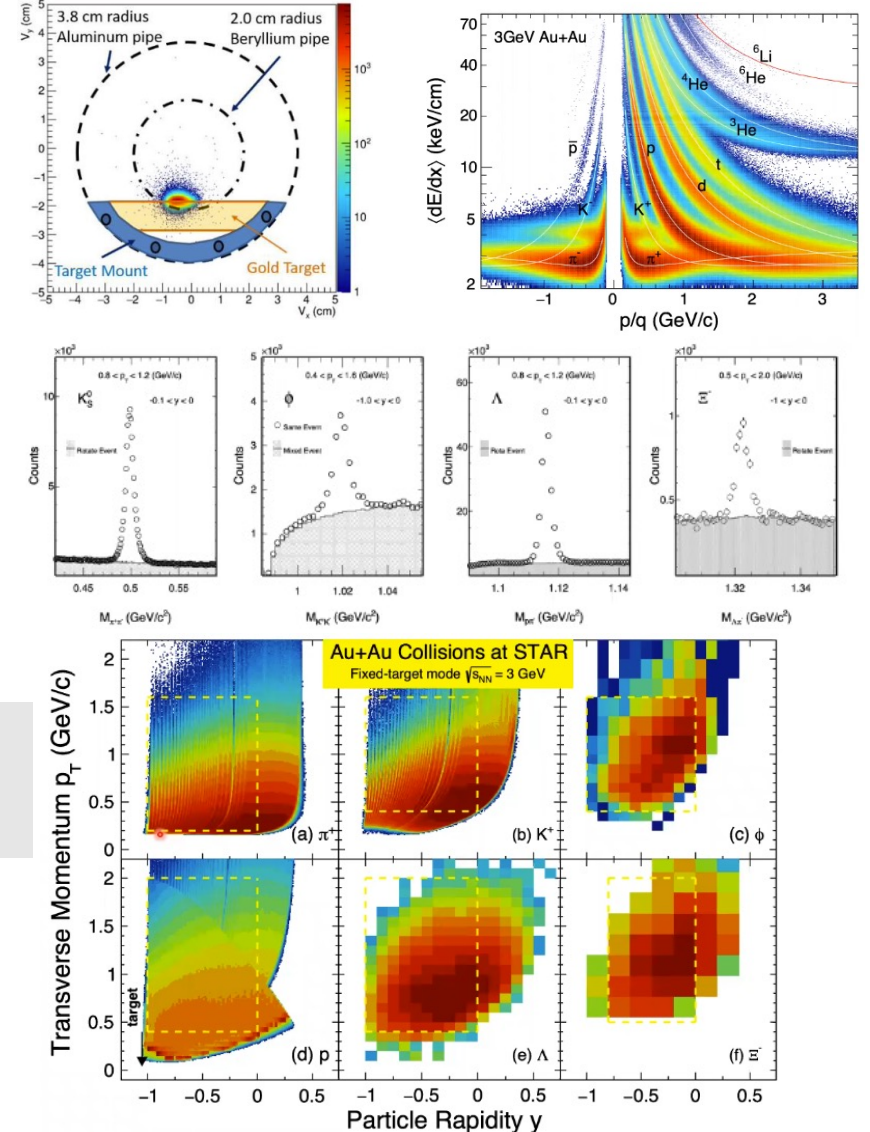
Fixed Target Mode at STAR



STAR: PLB
827, 137003
(2022)

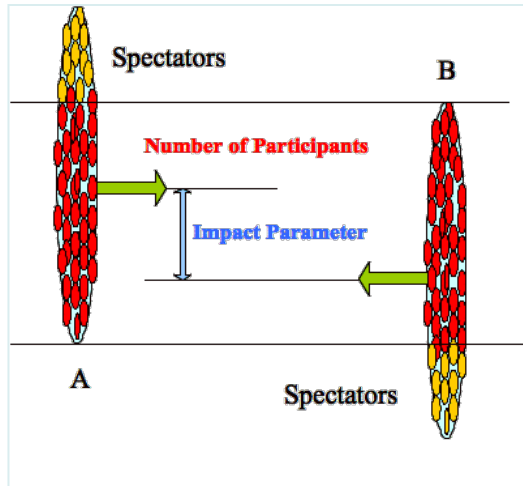
Au-Target:

- 250 μm thick gold foil
- 2 cm below nominal beam axis
- 2 m away from center of STAR



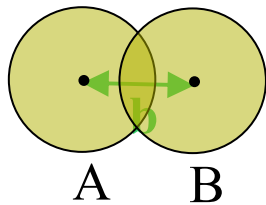


Collision Centrality

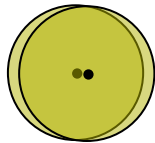


Measure of overlap of the two colliding nuclei
Central collisions: Maximum overlap
Peripheral collisions: Less overlap

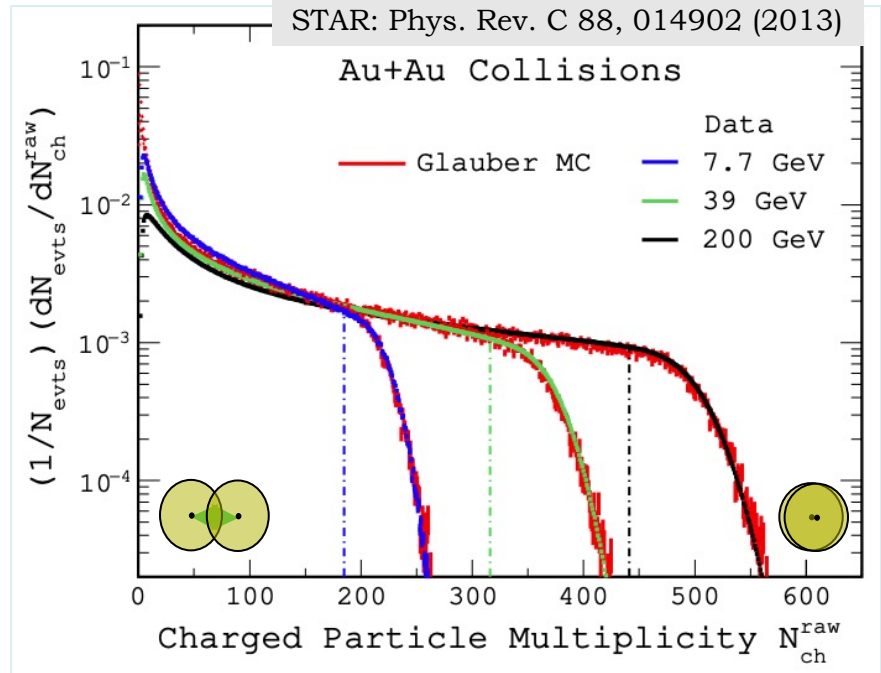
Glauber MC:
 N_{part} , N_{coll} , ...



Peripheral collisions
(Low multiplicity)



Central collisions
(High multiplicity)



Centrality classes are obtained as fractions of geometrical cross-section of the simulated multiplicity: 0-5%, 5-10%, 10-20%,... 70-80%



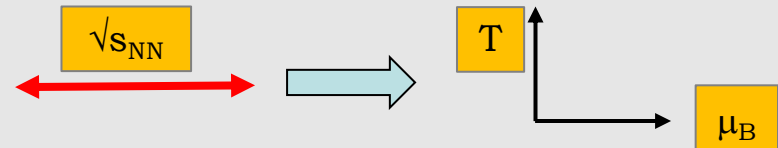
Outline

- Introduction
- Experimental Detail
- Results (from Beam Energy Scan)
- Summary

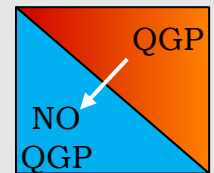


Beam Energy Scan: What to Look For?

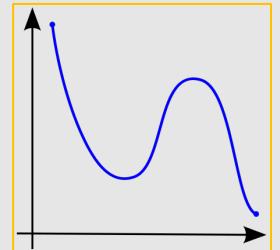
- Vary the collision energy (access various regions of phase diagram)



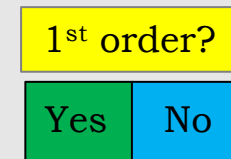
- Look for the turn-off of the established QGP signatures (evidence of phase boundary)



- Look for the non-monotonic behavior of fluctuations observable (evidence of critical point)

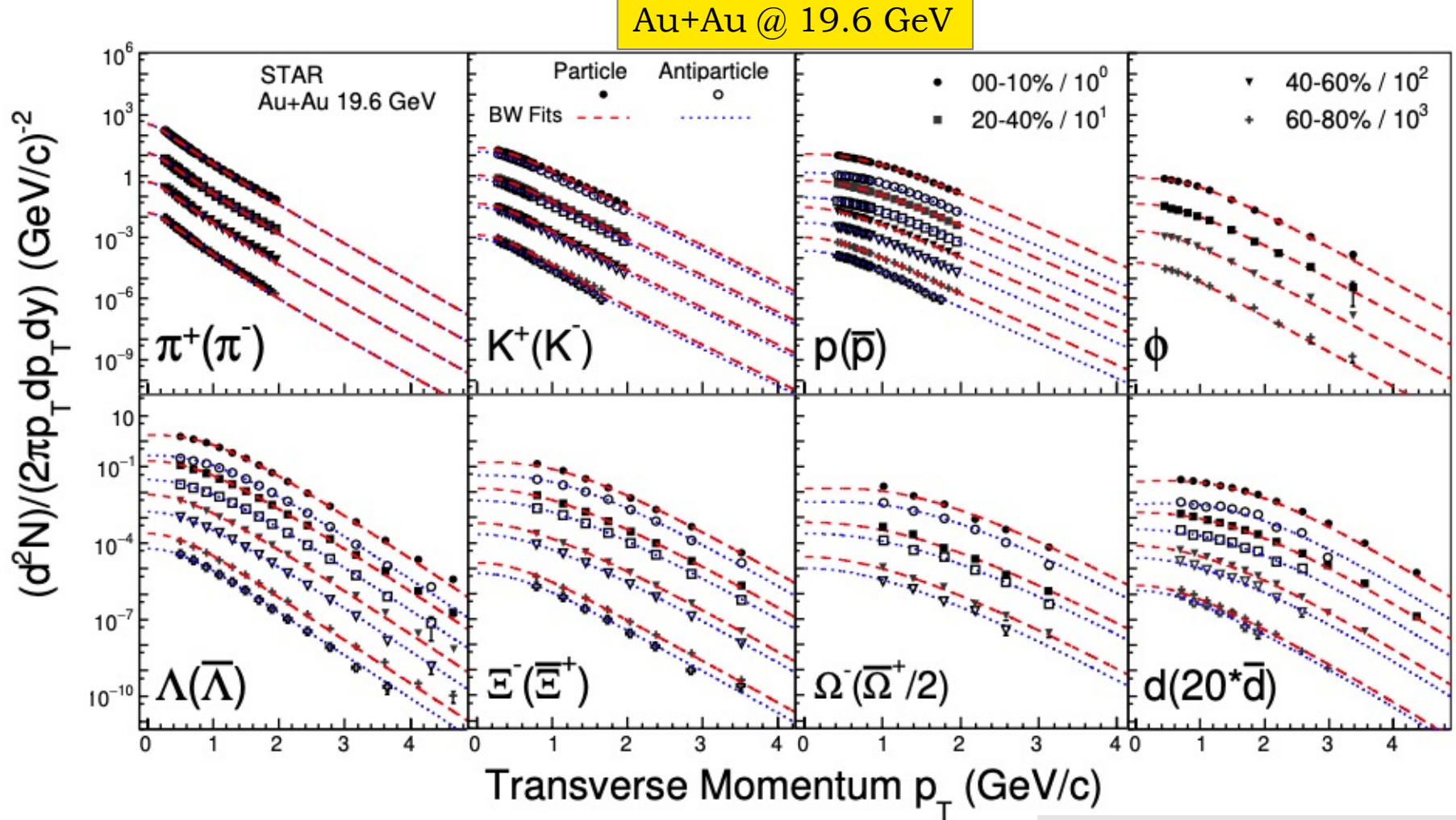


- Look for the suggested signatures of first-order phase transition





Identified Hadrons Invariant Yields



STAR: PRC 93, 021903 (2016)

STAR: PRC 96, 044904 (2017)

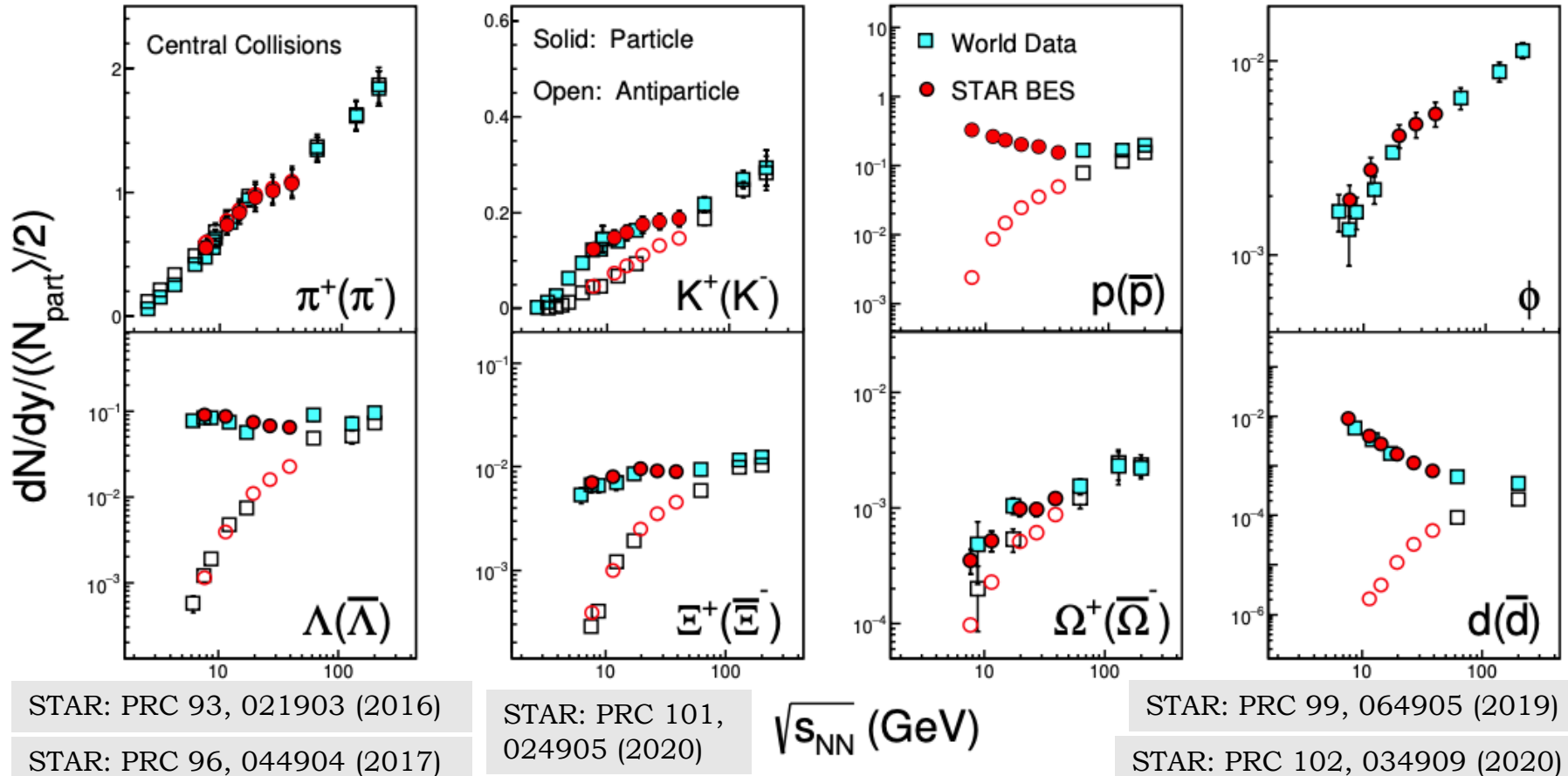
Integrating: dN/dy , $\langle p_T \rangle$

STAR: PRC 99, 064905 (2019)

STAR: PRC 102, 034909 (2020)



Energy Dependence of Yields

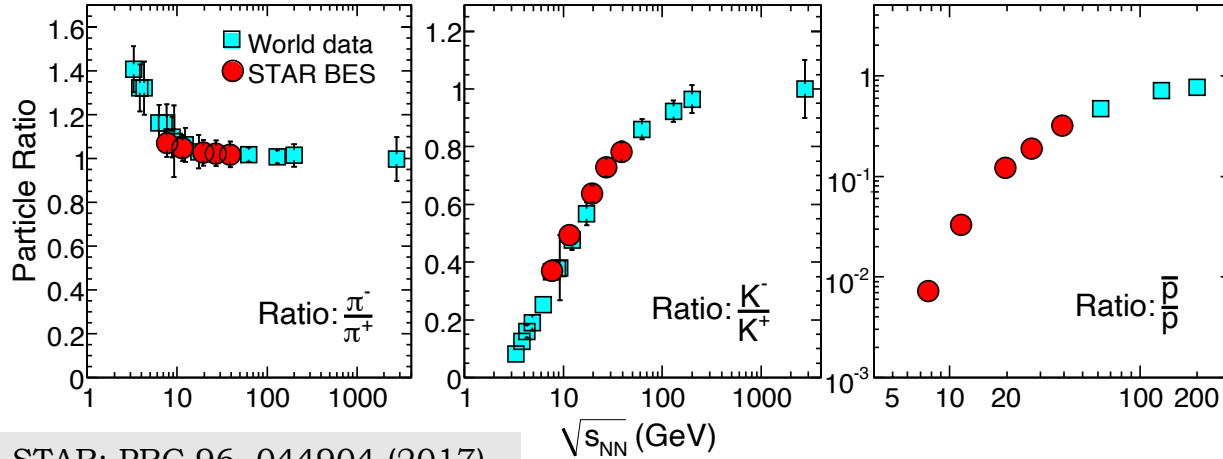


In general: Yields increase with increasing energy

Baryons: Yields at lower energies - higher compared to antibaryons
=> *Baryon stopping at midrapidity*



Particle Yield Ratios

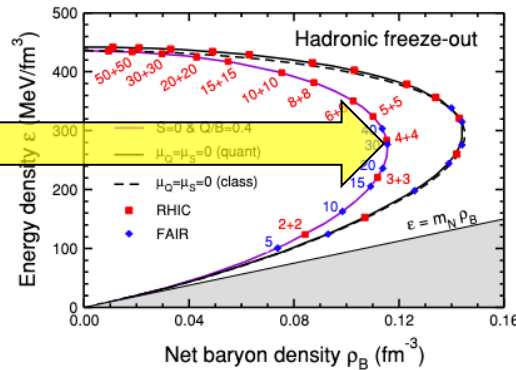
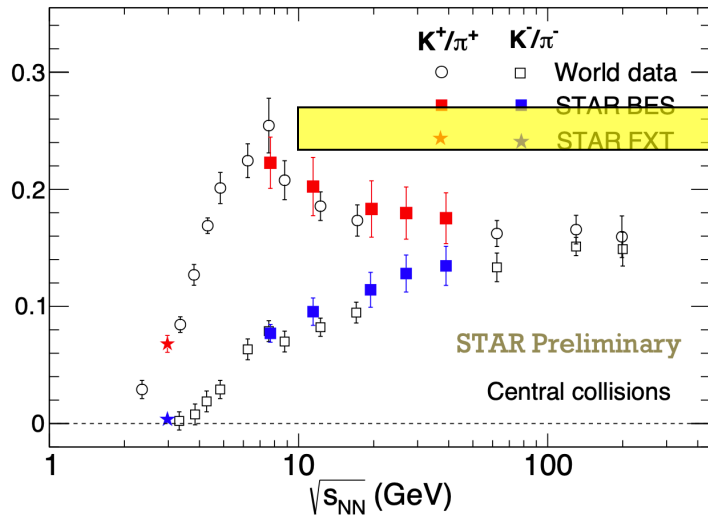


At low $\sqrt{s_{NN}}$, dN/dy :

$\pi^- > \pi^+$ [isospin and resonance decays such Δ baryons]

$K^+ > K^-$ [associated production, $NN \rightarrow KYN$, $pN \rightarrow KY$]

$p > \bar{p}$ [baryon stopping at midrapidity]



J. Randrup and J. Cleymans
PRC 74, 047901 (2006)

K/π : Peak corresponds to the energy having maximum net baryon density

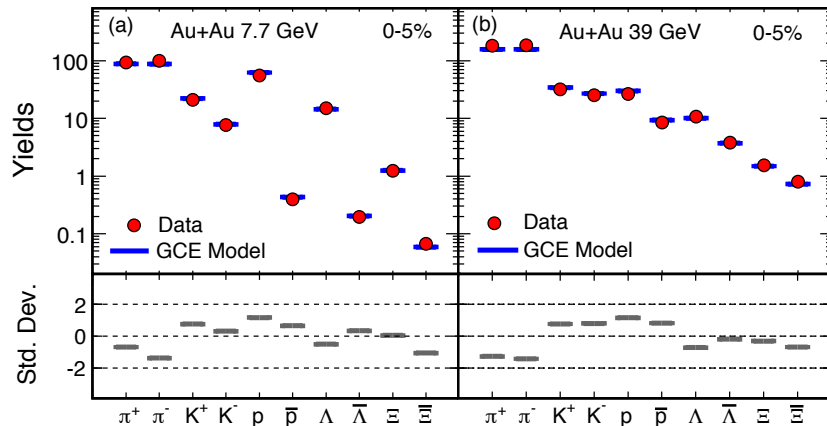


Chemical Freeze-out

Inelastic collisions cease
Chemical composition or
Particle ratios get fixed

$$n = \frac{1}{V} \frac{\partial(T \ln Z)}{\partial \mu} = \frac{VT m_i^2 g_i}{2\pi^2} \sum_{k=1}^{\infty} \frac{(\pm 1)^{k+1}}{k} \left(e^{\beta k \mu_i} \right) K_2 \left(\frac{km_i}{T} \right)$$

Dynamics characterized by:
Temperature T_{ch} and baryon
chemical potential μ_B



(T_{ch}, μ_B) points in phase diagram define
accessible region by the experiments

Statistical Thermal model:

- ❑ Assumes non-interacting hadrons and resonances
- ❑ Assumes thermodynamically equilibrium system
- ❑ Ensembles :

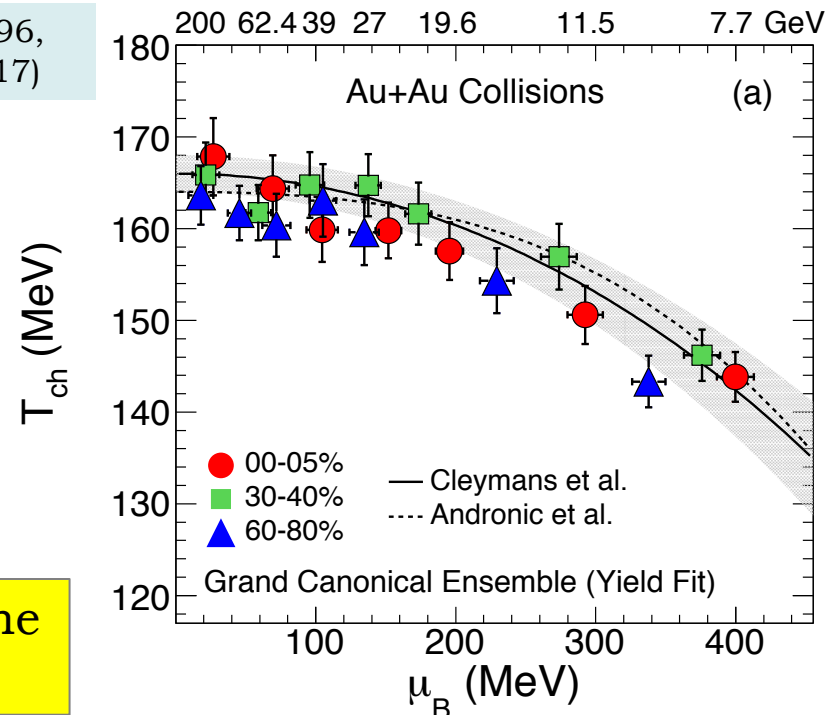
Grand Canonical - average conservation of B, S, Q

Strangeness Canonical - exact conservation of S

Canonical - exact conservation of B, S, and Q

S. Wheaton et al., *Comp.Phys. Comm.* **180**, 84 (2009).

STAR: PRC 96,
044904 (2017)





Kinetic Freeze-out

Elastic collisions cease
Momentum distributions
of particles get fixed

$$\frac{dN}{p_T dp_T} \propto \int_0^R r dr m_T I_0 \left(\frac{p_T \sinh \rho(r)}{T_{kin}} \right) \times K_1 \left(\frac{m_T \cosh \rho(r)}{T_{kin}} \right)$$

Dynamics characterized by:
Temperature T_{kin} and radial
flow velocity $\langle \beta \rangle$

Blast wave model:

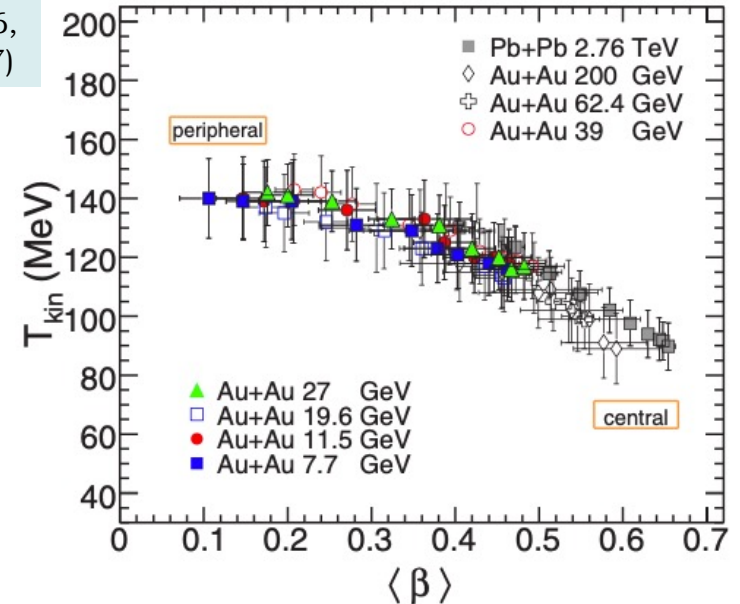
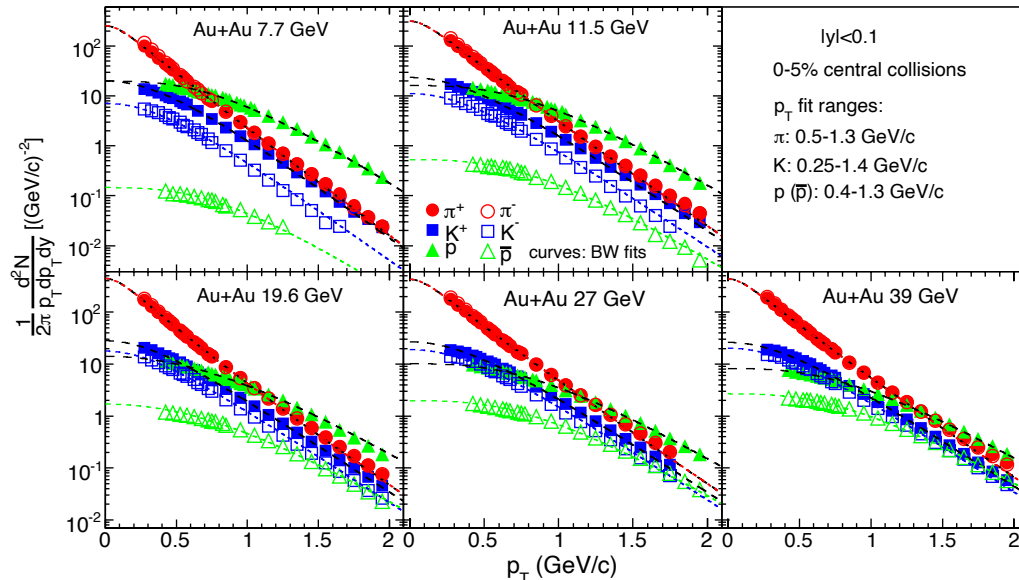
- Hydrodynamic based model
- Assumes particles are locally thermal at a kinetic freeze-out temperature and moving with a common radial flow velocity

E. Schnedermann, et al. PRC 48, 2462 (1993).

I_0, K_1 : Modified Bessel functions
 $\rho(r) = \tanh^{-1} \beta$
 r/R : relative radial position

β : transverse radial flow velocity
 T_{kin} : Kinetic freeze-out temp.
 R : radius of fireball

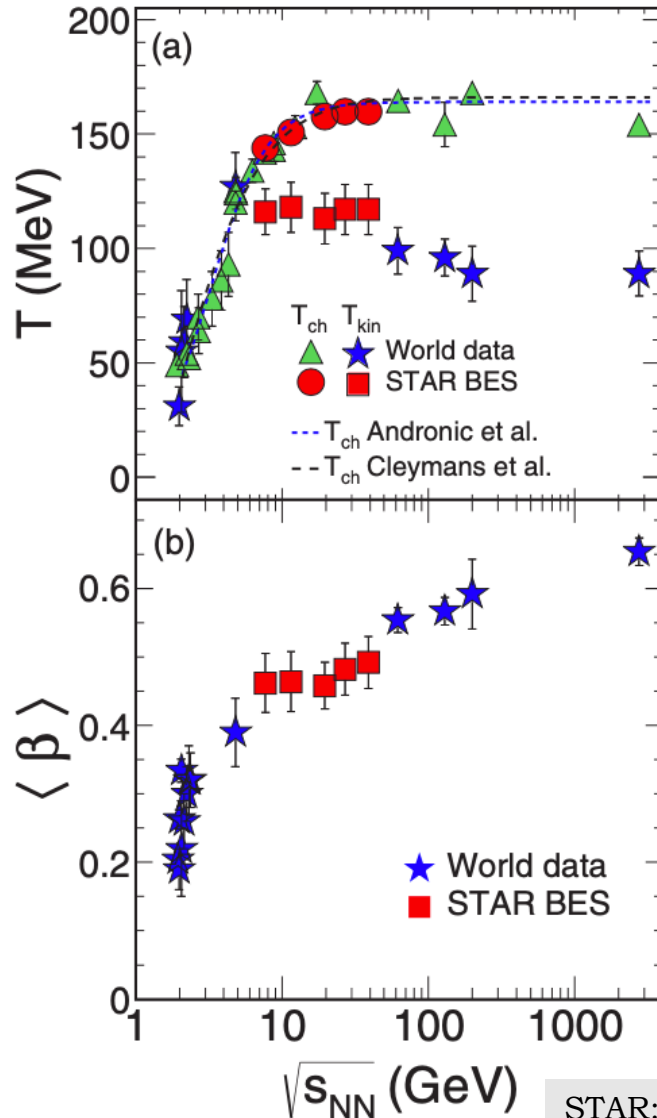
STAR: PRC 96,
044904 (2017)



T_{kin} and $\langle \beta \rangle$ are anti-correlated



Freeze-out Dynamics



STAR: PRC 96, 044904 (2017)

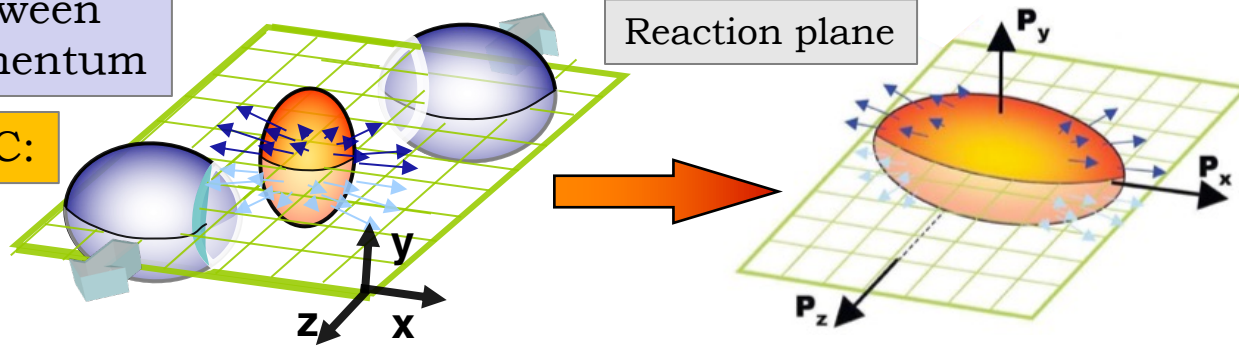
- ✓ Collectivity increases with beam energy for central collisions
- ✓ Chemical Freeze-out temperature increases and then saturates with beam energy
- ✓ Kinetic Freeze-out temperature decreases with beam energy for central collisions
- ✓ Gap between chemical and kinetic freeze-out temperatures increases with beam energy:
Suggests system interacts for longer duration at higher energy collisions



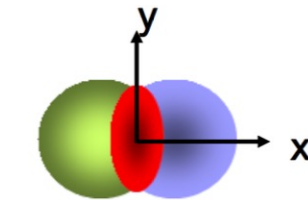
Collectivity

Correlation between space and momentum

Non-central HIC:

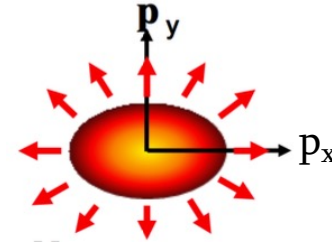


Initial spatial anisotropy



$$\varepsilon = \frac{\langle y^2 \rangle - \langle x^2 \rangle}{\langle y^2 \rangle + \langle x^2 \rangle}$$

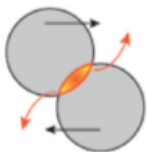
$$\phi = \tan^{-1} \left(\frac{p_y}{p_x} \right)$$



Final momentum anisotropy

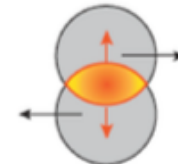
$$v_2 = \left\langle \frac{p_x^2 - p_y^2}{p_x^2 + p_y^2} \right\rangle$$

$$E \frac{dN^3}{d^3p} = \frac{1}{2\pi} \frac{d^2N}{p_t dp_t dy} (1 + 2v_1 \cos(\phi - \Psi_R) + 2v_2 \cos(2(\phi - \Psi_R) + \dots))$$



Directed flow

Elliptic flow

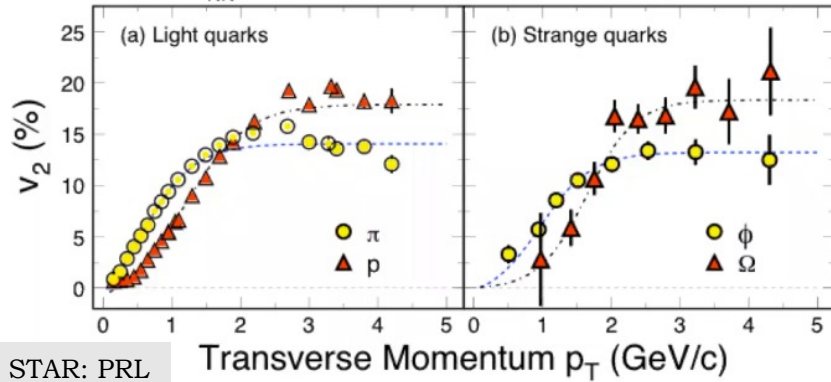


Related to initial/final conditions, EOS

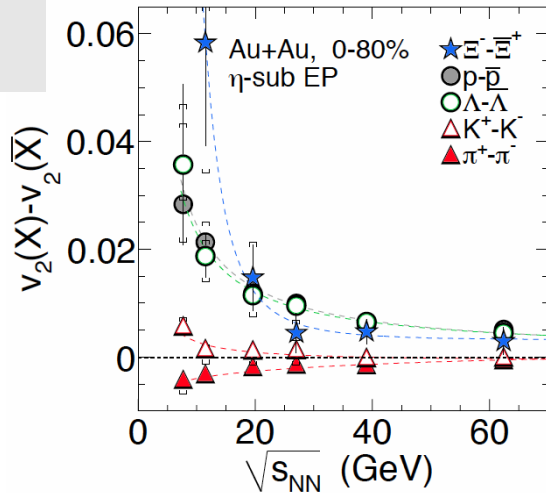


Partonic Collectivity Vs. \sqrt{s}_{NN}

$\sqrt{s}_{NN} = 200$ GeV $^{197}\text{Au} + ^{197}\text{Au}$ Collisions at RHIC



STAR: PRL
116,
062301
(2016)

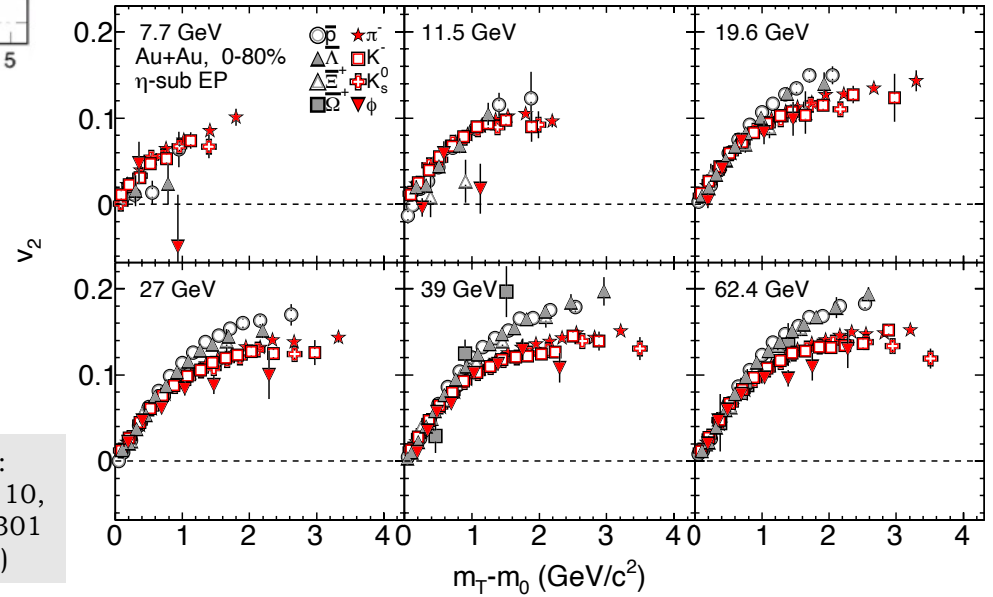


STAR:
PRL 110,
0142301
(2013)

Significant v_2 difference b/w particles and antiparticles at low \sqrt{s}_{NN} : NCQ scaling would be broken

Intermediate p_T :

- Baryon-meson separation: signature of partonic collectivity (QGP)
- NCQ-scaled v_2 : baryons & mesons follow single trend (QGP)



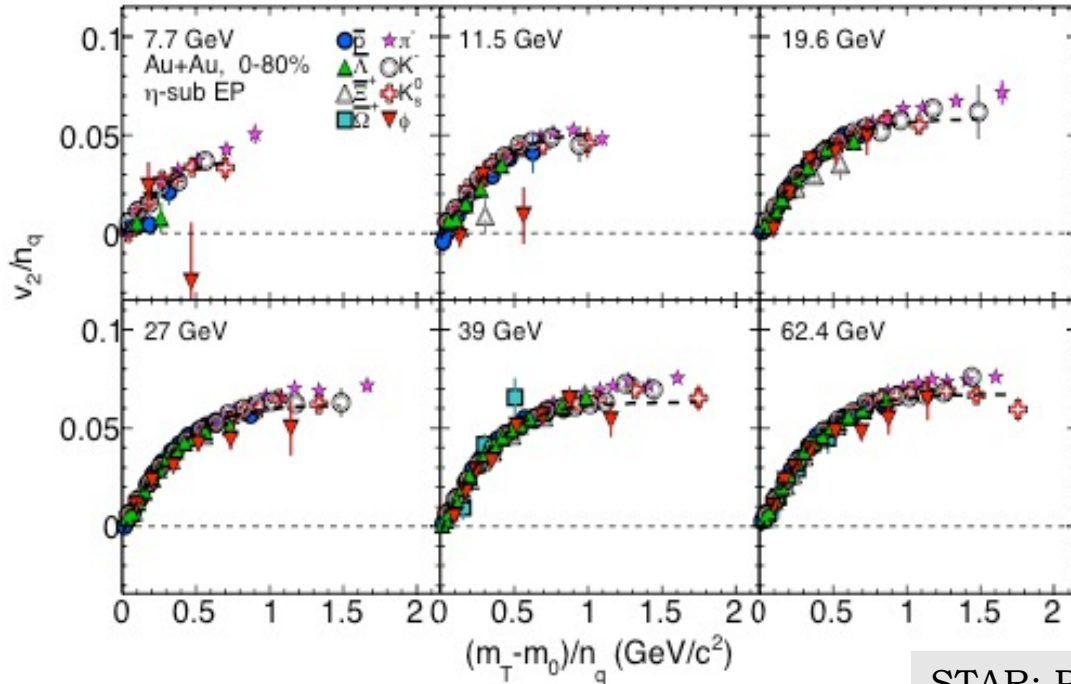
$\sqrt{s}_{NN} < 19.6$ GeV: No significant baryon-meson separation

low \sqrt{s}_{NN} : partonic collectivity signals missing

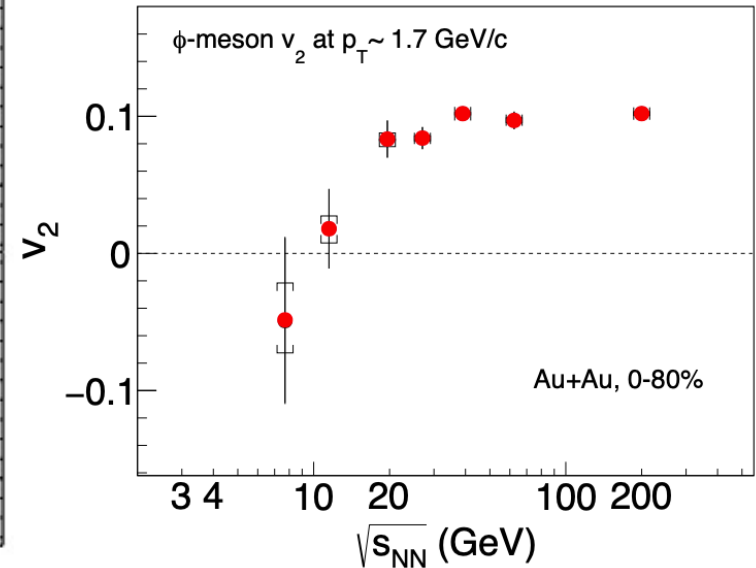


ϕ -meson v_2

ϕ -meson: least affected by the hadronic rescattering
 \Rightarrow reflects initial evolution of the system



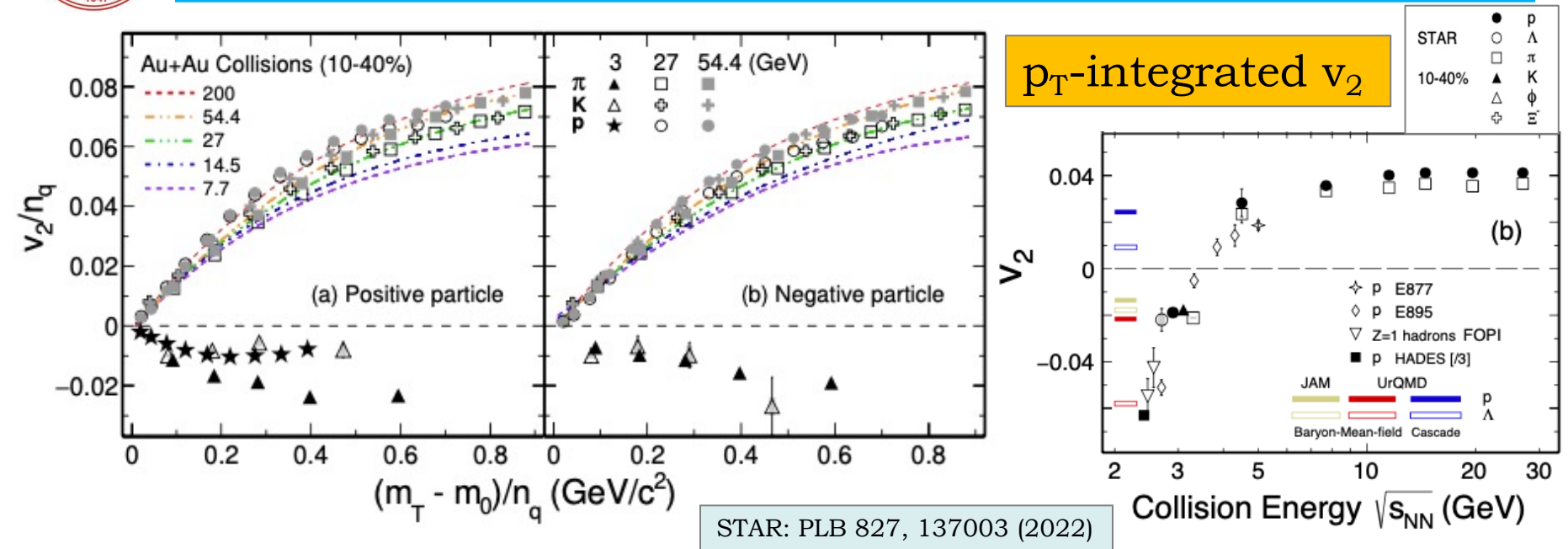
STAR: PRL 110, 0142301 (2013)



$\sqrt{s_{NN}} < 19.6$ GeV: ϕ -meson v_2 deviates and tends to zero
 -- Hadronic interactions dominate



Elliptic Flow at Very Low $\sqrt{s_{NN}}$



$\sqrt{s_{NN}} = 3 \text{ GeV: } v_2/n_q < 0$

\Rightarrow different properties of matter produced compared to higher $\sqrt{s_{NN}}$

Positive $v_2 \Rightarrow$ Early strong partonic expansion

Negative $v_2 \Rightarrow$ Weaker pressure gradient and shadowing of the spectators

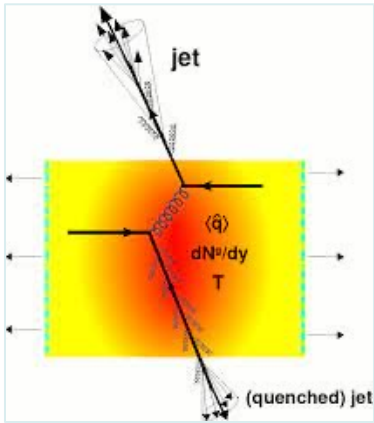
JAM and UrQMD (with baryonic mean-field): Explain the negative v_2

\Rightarrow Baryonic interactions are the dominant degrees of freedom



Jet Quenching

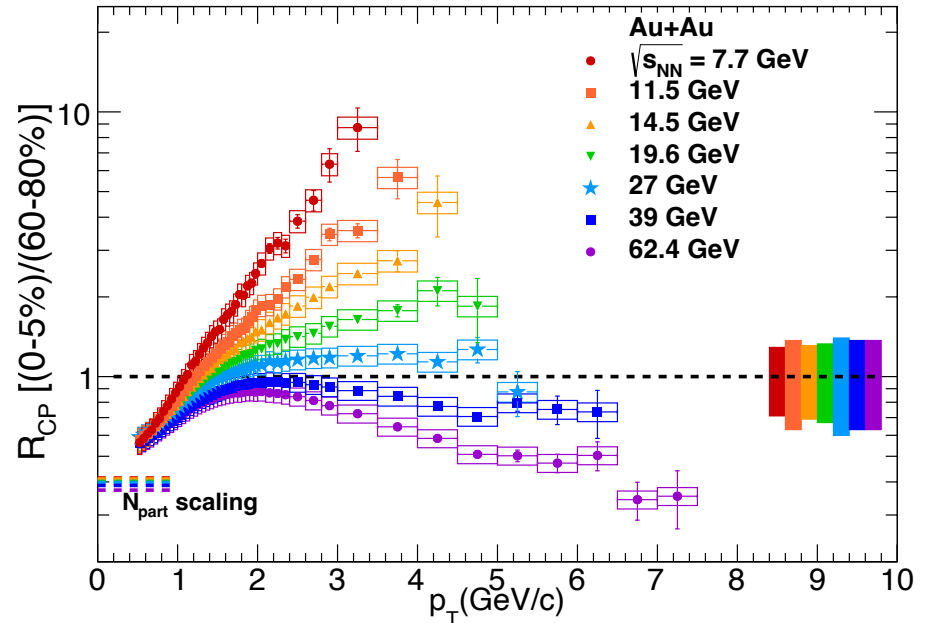
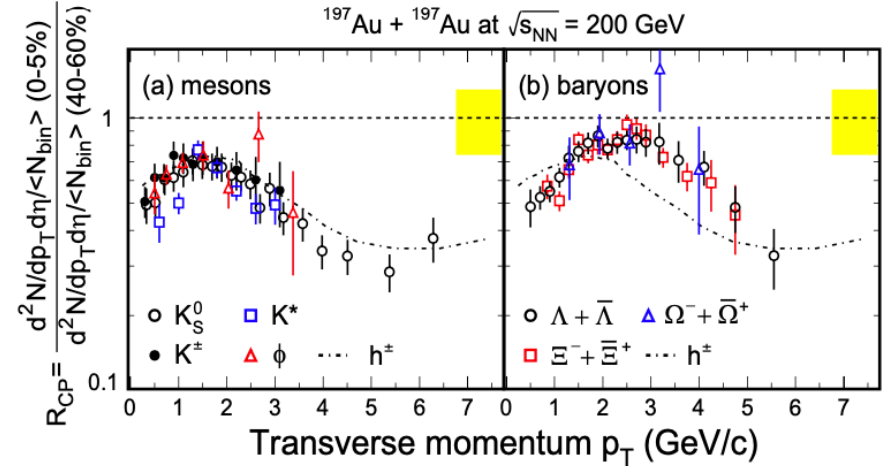
$$R_{CP} = \left[\frac{d^2 N^{\text{central}} / dp_T dy}{d^2 N^{\text{peripheral}} / dp_T dy} \right] \left[\frac{N_{\text{bin}}^{\text{peripheral}}}{N_{\text{bin}}^{\text{central}}} \right]$$



200 GeV Au+Au collisions:
Suppression at high- p_T –
Energy loss of partons in the dense QGP medium

STAR: PRL 121, 032301 (2018)

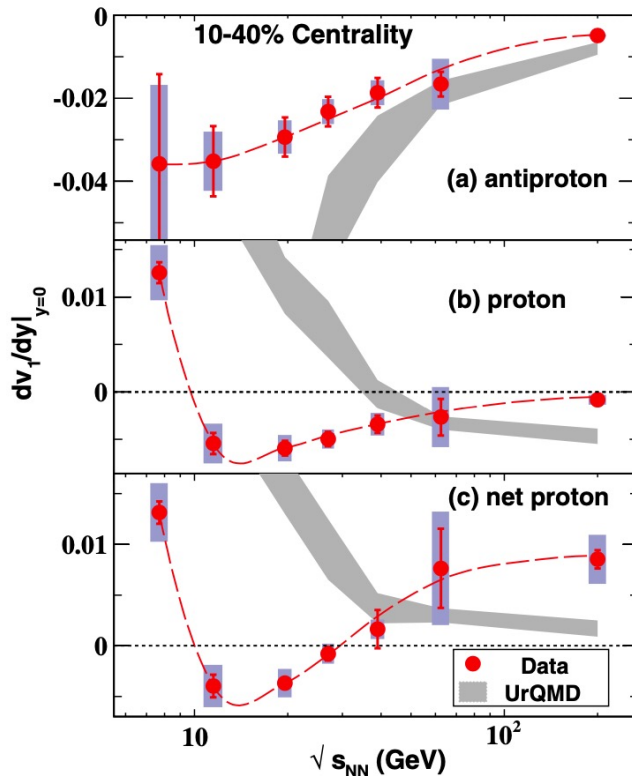
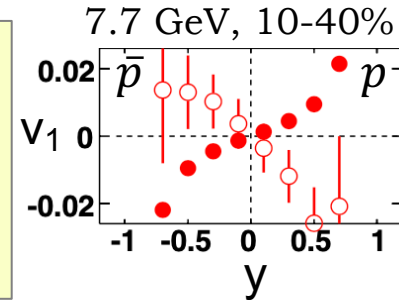
Expect at low $\sqrt{s_{NN}}$:
Vanishing of high- p_T suppression – due to low energy density or no QGP formation



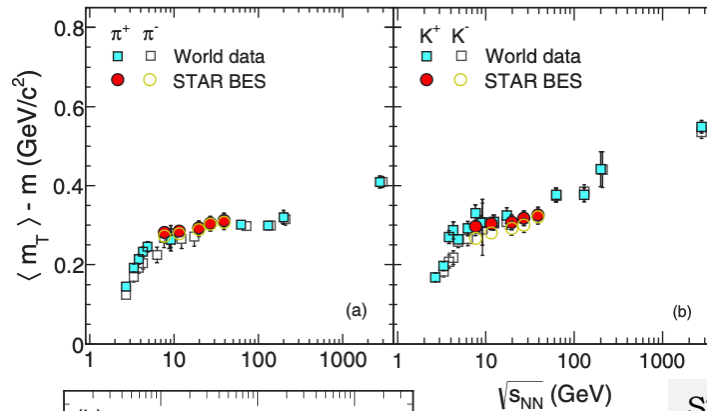


Directed Flow

- Collective sideways deflection of particles
 - Change of sign in the slope of directed flow (dv_1/dy) of baryons or net-baryons – softening of EOS/first order phase transition
- H. Stoecker, NPA 750, 121 (2005)

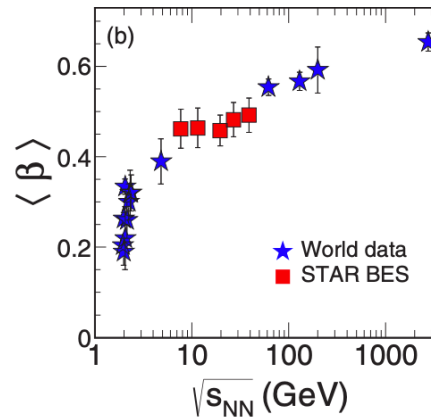


STAR: PRL 112, 162301 (2014)



Thermal excitation in transverse direction

STAR: PRC 96, 044904 (2017)



Radial flow velocity

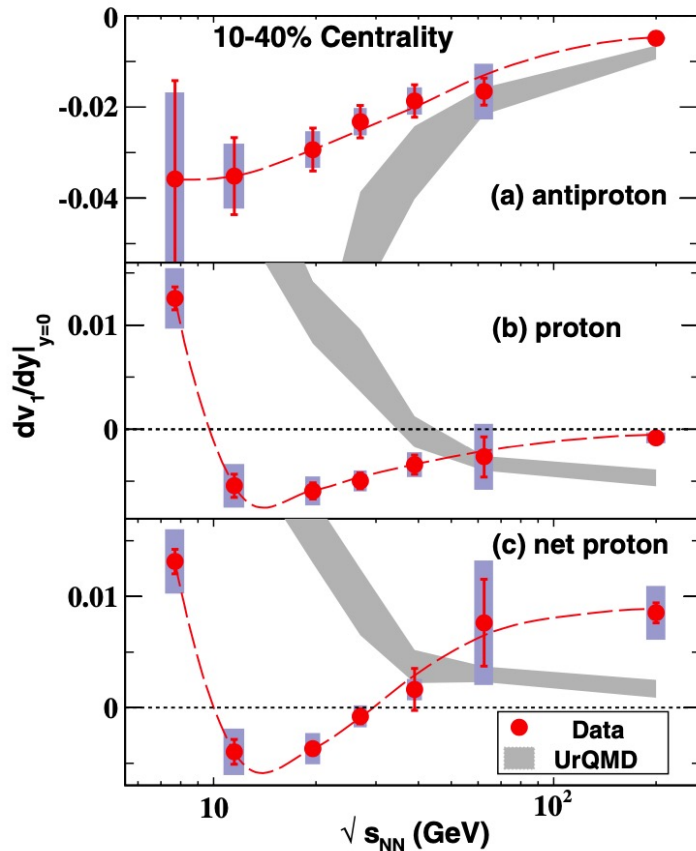
Mixed phase formation if the system undergoes 1st order phase transition



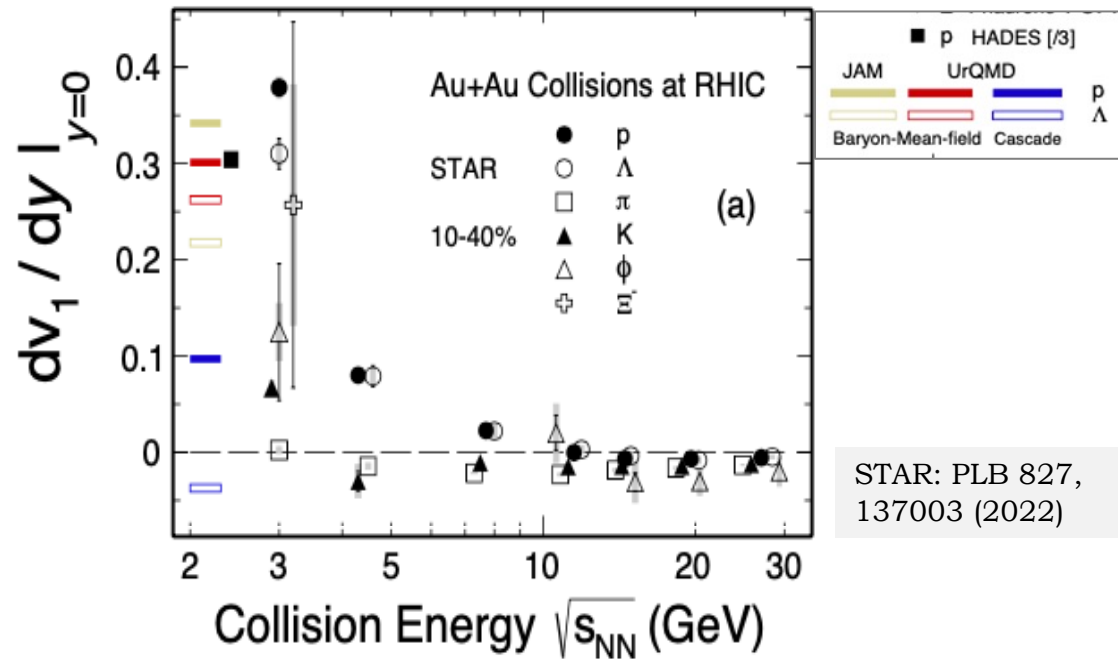
Directed Flow

High $\sqrt{s_{NN}}$ (partonic collectivity dominates): Negative $dv_1/dy \rightarrow 0$

Low $\sqrt{s_{NN}}$: Positive $dv_1/dy \Rightarrow$ different properties of matter



STAR: PRL 112, 162301 (2014)



STAR: PLB 827, 137003 (2022)

Low $\sqrt{s_{NN}}$: baryonic interactions dominate!



Search for Critical Point

- Strong interactions: Baryon (B), Charge (Q) and Strangeness (S) numbers are conserved.
- Fluctuations in the conserved quantities – give information on the critical point
- Enhanced fluctuations at a given (T_{ch}, μ_B) point in the phase diagram – suggest critical point

CO₂ near liquid-gas transition



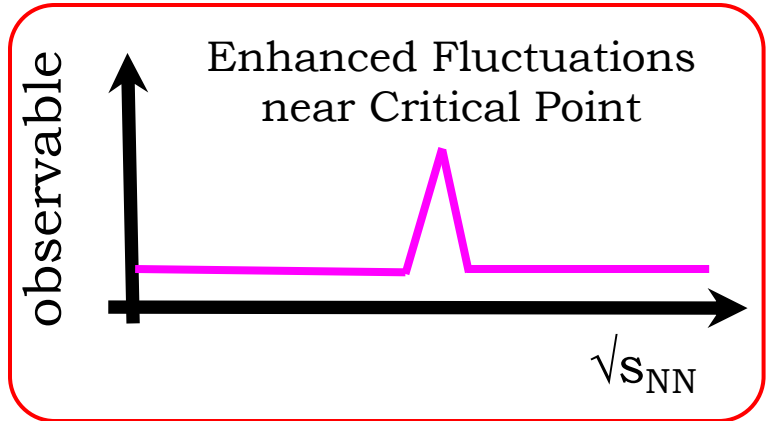
$T > T_c$

$T \sim T_c$

$T < T_c$

Critical Opalescence

T. Andrews.
Phil. Trans.
Royal Soc.,
159:575,
1869



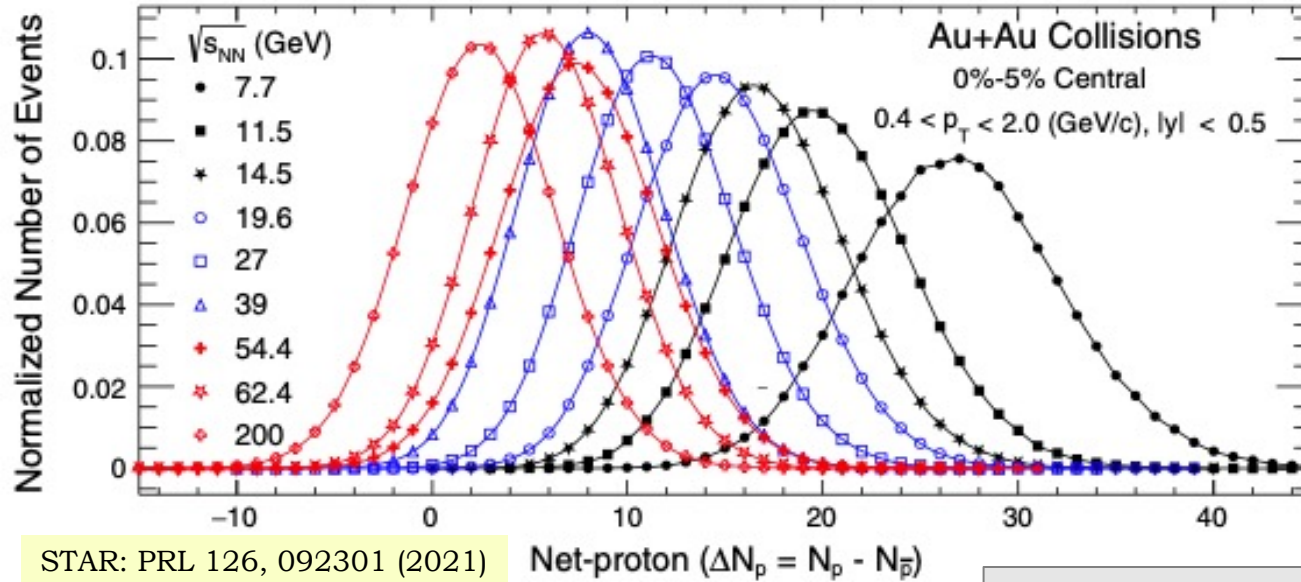
Fluctuations can be measured:
Through higher order
moments/cumulants from the
distributions of **net-B**, net-Q, net-S



Search for Critical Point

Event-by-event net-proton distributions

Good proxy of net-B



STAR: PRL 126, 092301 (2021)

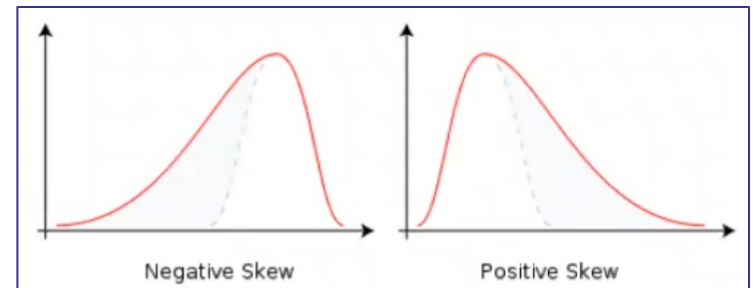
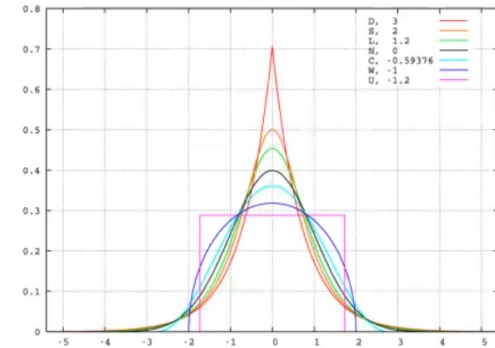
Net-proton ($\Delta N_p = N_p - N_{\bar{p}}$)

Moments	Value	Cumulants
Mean	$M = \langle N \rangle$	C_1
Variance	$\sigma^2 = \langle (\delta N)^2 \rangle$	C_2
Skewness	$S = \langle (\delta N)^3 \rangle / \sigma^3$	$C_3 / C_2^{3/2}$
Kurtosis	$\kappa = \frac{\langle (\delta N)^4 \rangle}{\sigma^4} - 3$	C_4 / C_2^2

Skewness (S):
Asymmetry

Characterized by:
Mean multiplicity
 $\langle N \rangle, \langle \delta N \rangle = N - \langle N \rangle$

Kurtosis (κ):
Sharpness





Search for Critical Point

- Correlation length (ζ) -- Diverges near critical point
- Higher moments -- most sensitive to the correlation length

M. A. Stephanov, PRL 102, 032301 (2009)

Non-monotonic behavior of higher moments of conserved quantities -- experimental signature of critical point

M. A. Stephanov et al., PRD 60, 114028 (1999)

M. A. Stephanov, PRL 107, 052301 (2011)

Ratios of cumulants – cancelation of volume effects and related to the susceptibilities ratios computed in the lattice QCD

Moments -order	Value	Susceptibilities ratios
2 nd order	$\sigma^2/M = C_2/C_1$	χ_2/χ_1
3 rd order	$S\sigma = C_3/C_2$	χ_3/χ_2
4 th order	$\kappa\sigma^2 = C_4/C_2$	χ_4/χ_2

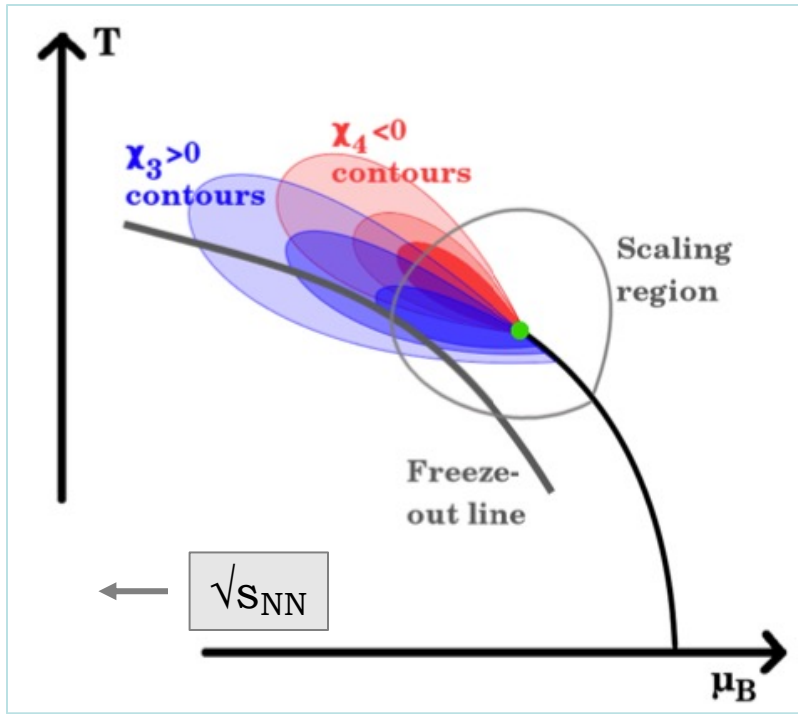
R.V. Gavai et al., PLB 696, 459 (2011)

B. Stokic et al., , PLB 673, 192 (2009)

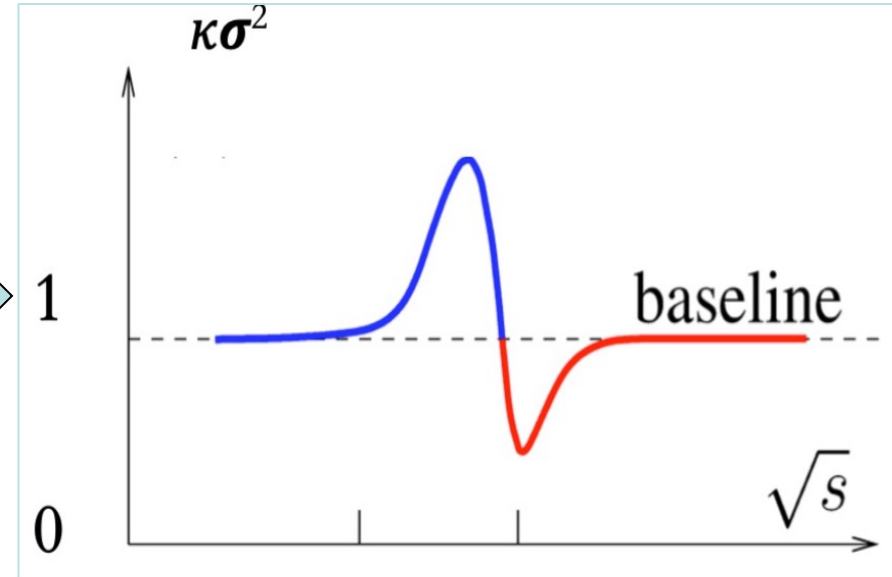
Experimental observable – directly compared to theory!



Search for Critical Point: Theory



M. A. Stephanov, PRL 107, 052301 (2011)

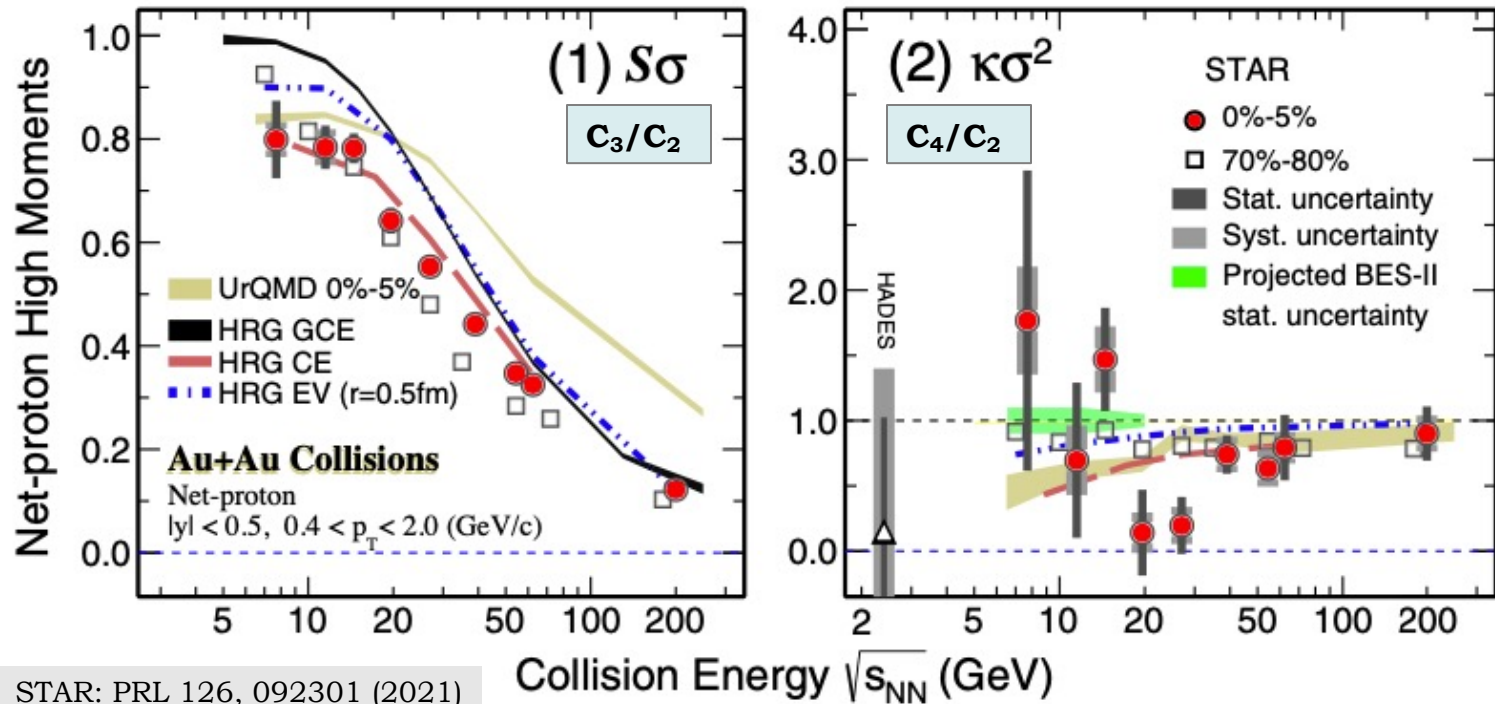


J. W. Chen et al., PRD 93, 034037 (2016)

- “Oscillating pattern” expected for critical point
- Actual shape depends on the accessible “critical region” (finite size and time of the system created in heavy-ion collisions)



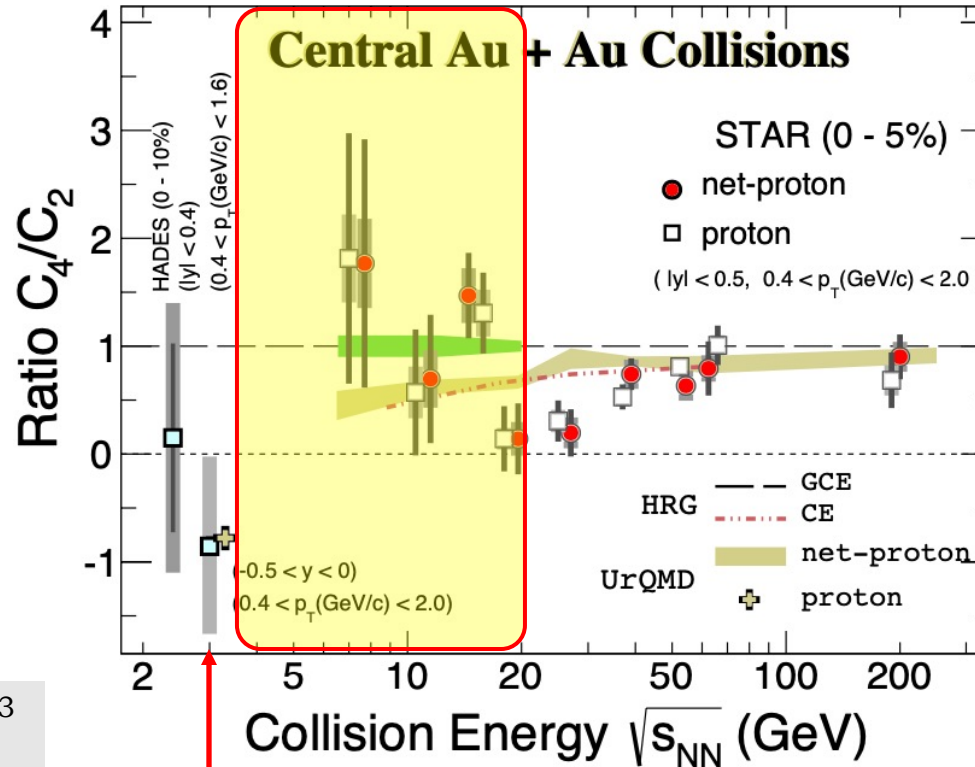
Search for Critical Point: Experiment



- Central collisions: non-monotonic energy dependence, 3.1σ effect for 4th order
- Deviation from Poisson baseline
- UrQMD, CE (no CP, include baryon conservation) – decrease monotonically towards low $\sqrt{s_{NN}}$



Search for Critical Point: low $\sqrt{s_{NN}}$



STAR: PRL 128, 202303
(2022)

STAR: PRL 126, 092301
(2021)

STAR: PRC 104, 024902
(2021)

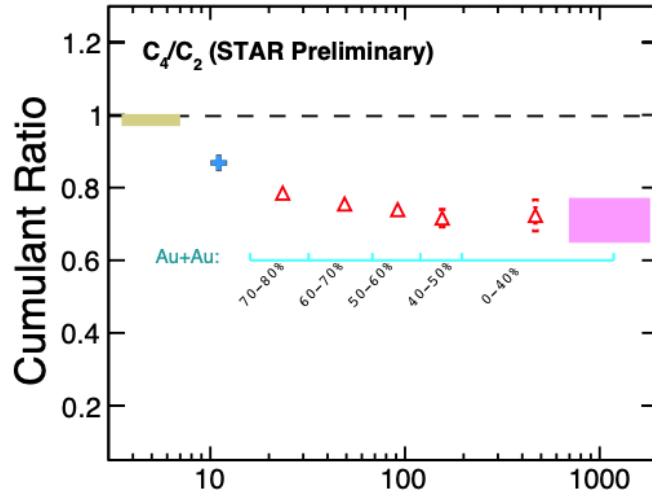
C_4/C_2 ratio for proton at 3 GeV - below Poisson

-- consistent with fluctuations driven by baryon number conservation at high baryon density

Critical point, if exists, could likely be at $\sqrt{s_{NN}} > 3$ GeV
 – BES-II ($\sqrt{s_{NN}} = 3 - 19.6$ GeV, $\mu_B = 206 - 720$ MeV)

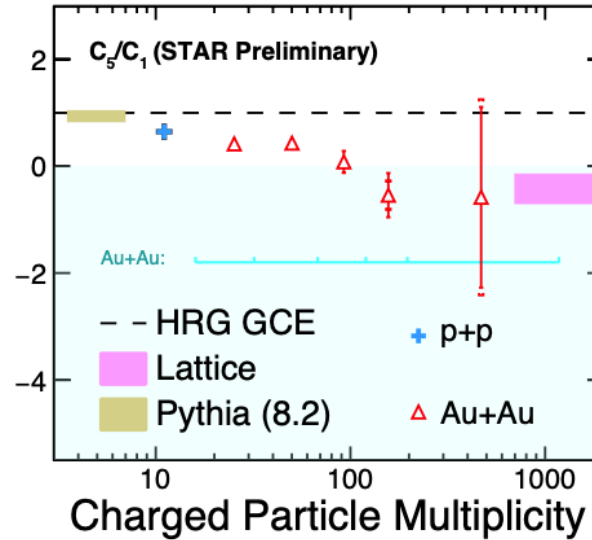


Higher-order Net-proton Cumulants

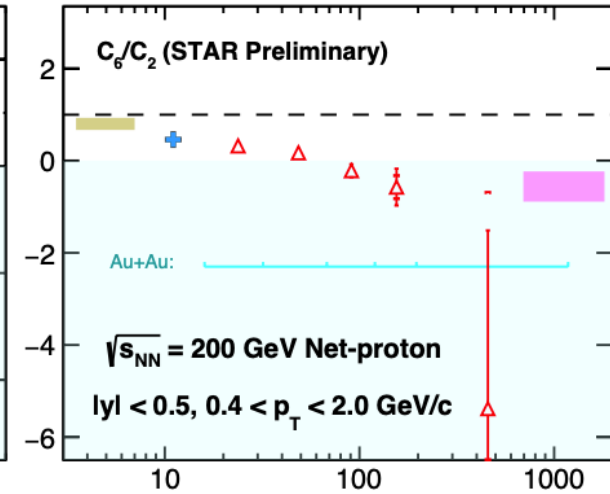


STAR: PRL 127, 262301 (2021)

STAR: PRC 104, 024902 (2021)



STAR: QM2022



A. Bazavov et al. PRD 101, 074502 (2020)

pp 200 GeV: $C_4/C_2, C_5/C_1, C_6/C_2 > 0$

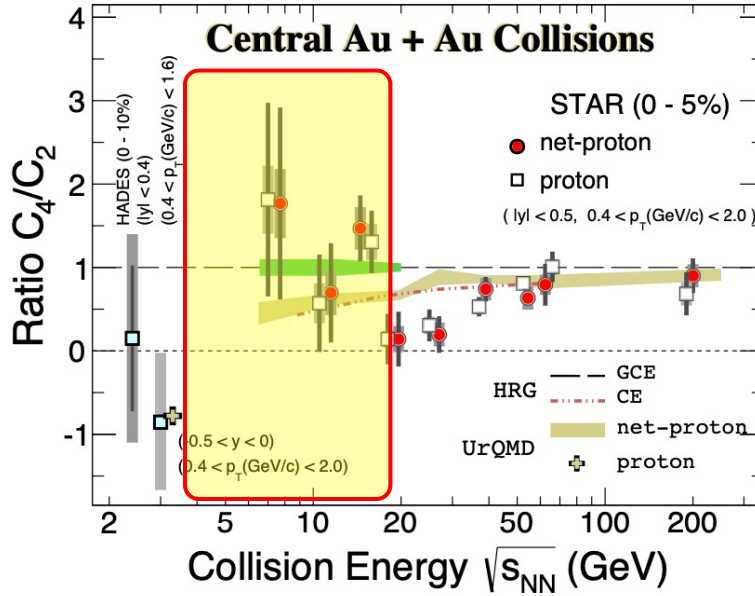
Lattice QCD (with **smooth crossover phase transition** of thermalized medium at $\mu_B = 0$): predicts $C_5/C_1, C_6/C_2 < 0$

Au+Au 200 GeV (central collisions): Consistent with lattice QCD result

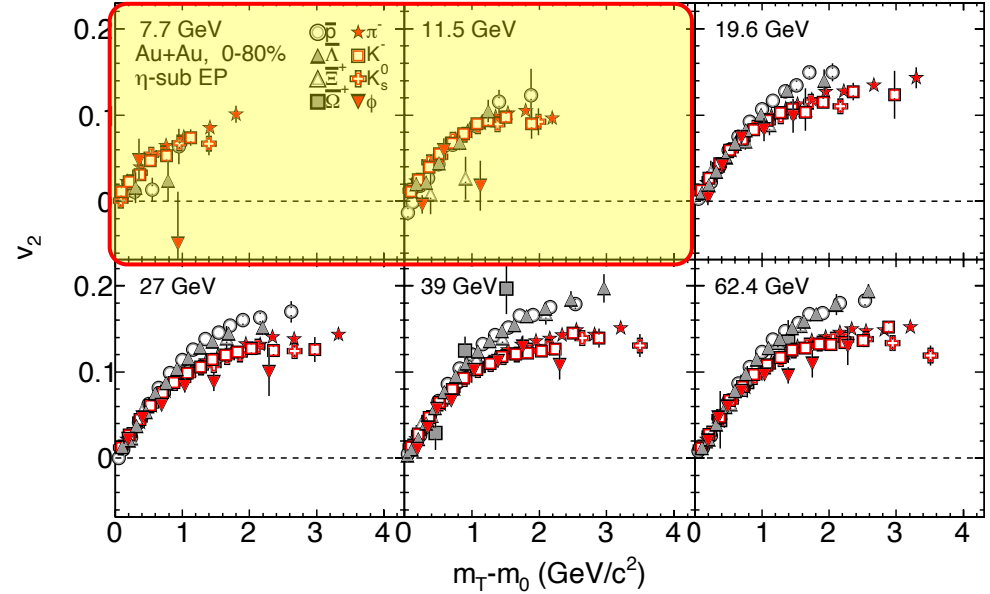
Direct evidence of QGP formation in 200 GeV central Au+Au collisions!



Beam Energy Scan-II and FXT



Hint of critical point!



Hint of turn-off of QGP signatures!

BES-I
Statistics:

$\sqrt{s_{NN}}$ (GeV)	Events (million)
7.7	4
11.5	8
19.6	17.3
27	33
39	111

High statistics required
for $\sqrt{s_{NN}} = 3 - 19.6 \text{ GeV}$

Achieve in BES-II
and FXT collisions!



Beam Energy Scan-II and FXT

BES-II, FXT and
200 GeV data:
2018-2021

Data collection
completed:

$\sqrt{s}_{NN} = 3 - 200 \text{ GeV}$
 $\mu_B = 25 - 720 \text{ MeV}$

FAIR: fixed-target

$\sqrt{s}_{NN} = 2.7 - 4.9 \text{ GeV}$
 $\mu_B = 560 - 753 \text{ MeV}$

NICA: Collider

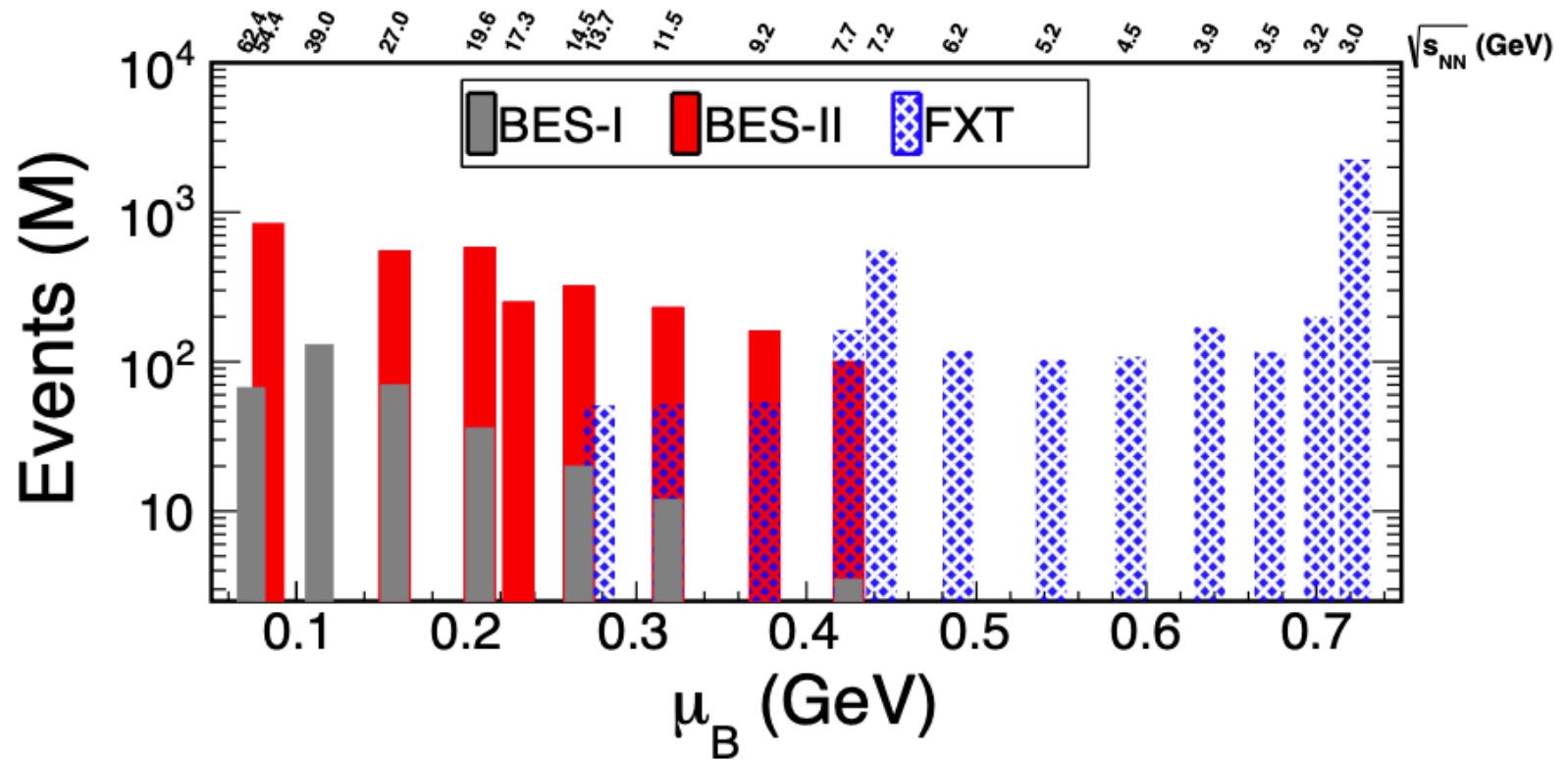
$\sqrt{s}_{NN} = 3.0-11.0 \text{ GeV}$
 $\mu_B = 327 - 720 \text{ MeV}$

All programs
complement
each other!

\sqrt{s}_{NN} (GeV)	Beam Energy (GeV/nucleon)	Collider or Fixed Target	$y_{\text{center of mass}}$	μ_B (MeV)	Run Time (days)	No. Events Collected (Request)	Date Collected
200	100	C	0	25	2.0	138 M (140 M)	Run-19
27	13.5	C	0	156	24	555 M (700 M)	Run-18
19.6	9.8	C	0	206	36	582 M (400 M)	Run-19
17.3	8.65	C	0	230	14	256 M (250 M)	Run-21
14.6	7.3	C	0	262	60	324 M (310 M)	Run-19
13.7	100	FXT	2.69	276	0.5	52 M (50 M)	Run-21
11.5	5.75	C	0	316	54	235 M (230 M)	Run-20
11.5	70	FXT	2.51	316	0.5	50 M (50 M)	Run-21
9.2	4.59	C	0	372	102	162 M (160 M)	Run-20+20b
9.2	44.5	FXT	2.28	372	0.5	50 M (50 M)	Run-21
7.7	3.85	C	0	420	90	100 M (100 M)	Run-21
7.7	31.2	FXT	2.10	420	0.5+1.0+ scattered	50 M + 112 M + 100 M (100 M)	Run-19+20+21
7.2	26.5	FXT	2.02	443	2+Parasitic with CEC	155 M + 317 M	Run-18+20
6.2	19.5	FXT	1.87	487	1.4	118 M (100 M)	Run-20
5.2	13.5	FXT	1.68	541	1.0	103 M (100 M)	Run-20
4.5	9.8	FXT	1.52	589	0.9	108 M (100 M)	Run-20
3.9	7.3	FXT	1.37	633	1.1	117 M (100 M)	Run-20
3.5	5.75	FXT	1.25	666	0.9	116 M (100 M)	Run-20
3.2	4.59	FXT	1.13	699	2.0	200 M (200 M)	Run-19
3.0	3.85	FXT	1.05	721	4.6	259 M -> 2B(100 M -> 2B)	Run-18+21



Beam Energy Scan-II and FXT

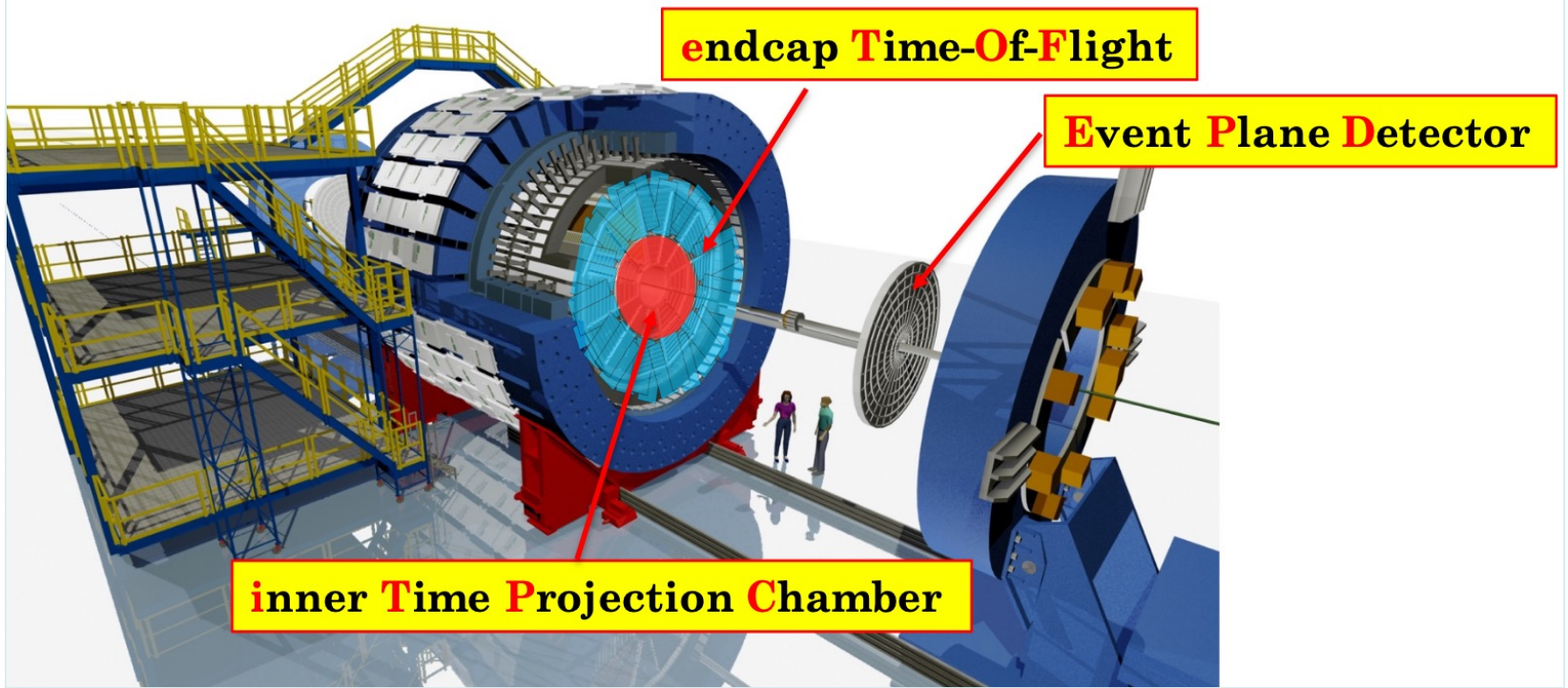


- Many fold increase in statistics compared to BES-I
- Fixed target extends the μ_B range above 700 MeV

In addition: Upgrades of STAR detectors –
iTPC, EPD, eTOF



STAR Upgrades BES-II

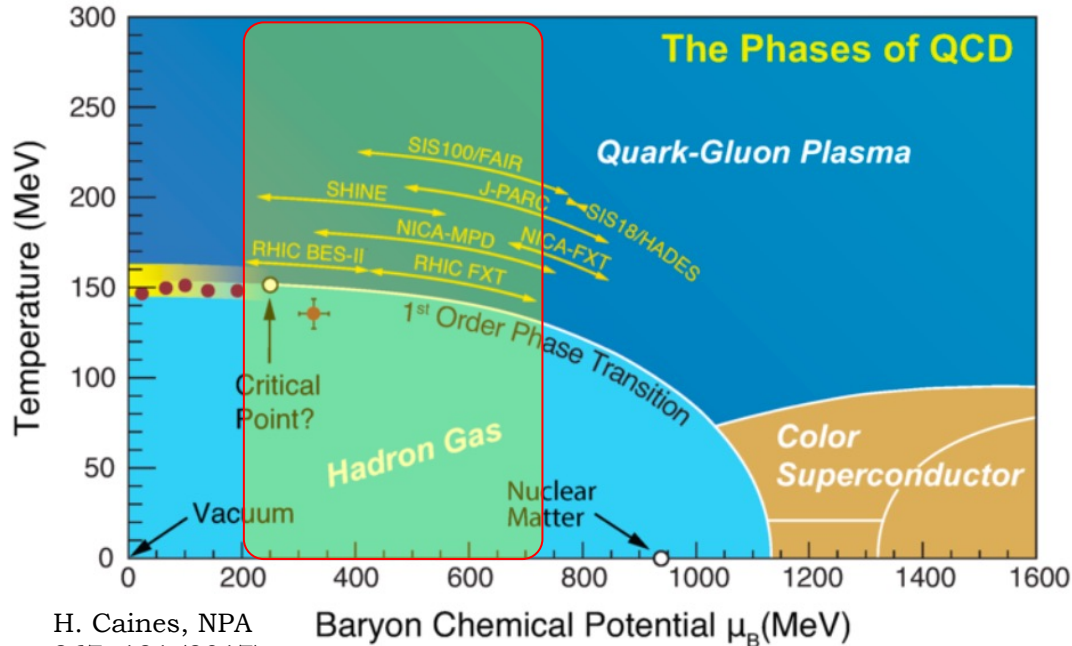


iTPC upgrade	EPD upgrade	eTOF upgrade
Continuous pad rows Replace all inner TPC sectors	Replace Beam Beam Counter	Add CBM TOF modules and electronics (FAIR Phase 0)
$ \eta < 1.5$ (was 1.0)	$2.1 < \eta < 5.1$	$-1.6 < \eta < -1.1$
$p_T > 60$ MeV/c (was 150 MeV/c)	Better trigger & b/g reduction	Extend forward PID capability
Better dE/dx resolution Better momentum resolution	Greatly improved Event Plane info (esp. 1 st -order EP)	Allows higher energy range of Fixed Target program
Fully operational in 2019	Fully operational in 2018	Fully operational in 2019



Summary

Low μ_B : Direct evidence of QGP formation and smooth crossover



BES-II and future facilities (FAIR, NICA) could help to consolidate the BES-I findings

CP, if exists:

$\sqrt{s_{NN}} = 3 \text{ -- } 19.6 \text{ GeV}$, $\mu_B = 206 \text{ -- } 720 \text{ MeV}$

Low $\sqrt{s_{NN}}$

($\sqrt{s_{NN}} = 3 \text{ GeV}$, $\mu_B = 720 \text{ MeV}$) :

Hadronic interactions
dominate

In between

($\sqrt{s_{NN}} = 3 \text{ -- } 19.6 \text{ GeV}$,
 $\mu_B = 206 \text{ -- } 720 \text{ MeV}$) :

Interesting trends:

- Hints of turn-off of QGP signatures
- Hints of 1st order phase transition
- Hints of critical point



Acknowledgements

STAR Collaboration and RHIC Operations

Discussions with Prof. B. Mohanty and
Dr. N. Sharma



Thank you very much for your
attention!

Back-up